UNIVERSIDADE DA BEIRA INTERIOR
Ciências

Transfection Efficiency of a Vector for Mitochondrial Gene Therapy

Rúben Joel Bispo Salvado

Dissertação para obtenção do Grau de Mestre em
Bioquímica
(2º ciclo de estudos)

Orientador: Professora Doutora Diana Costa
Coorientador: Professora Doutora Fani Sousa

Covilhã, outubro de 2014

"A book is made from a tree. It is an assemblage of flat, flexible parts (still called "leaves") imprinted with dark pigmented squiggles. One glance at it and you hear the voice of another person, perhaps someone dead for thousands of years. Across the millennia, the author is speaking, clearly and silently, inside your head, directly to you. Writing is perhaps the greatest of human inventions, binding together people, citizens of distant epochs, who never knew one another. Books break the shackles of time — proof that humans can work magic."

Carl Sagan (1934-1996)

Acknowledgments

First and foremost I offer my sincerest gratitude to my supervisors Prof. Diana Costa, PhD and Prof. Fani Sousa, PhD for all the help and support that they gave me during the execution and writing of this MSc dissertation. Without their knowledge and scientific insights, this dissertation would not have been possible.

I would also like to thank the biotechnology group, especially Prof. Ângela Sousa, PhD and Lúcia Amorim for helping me during the plasmid production and purification.

To the Endocrinology group, Eduarda Coutinho, Maria Inês Alvelos and Catarina Gonçalves for all the help and tips they gave me with the PCR and sequencing techniques.

Carlos Gaspar, and again Eduarda Coutinho, for the help they gave during the competent cell preparation and the transformation protocols.

Eng. Ana Paula Gomes and Catarina Ferreira for the assistance during the SEM and Confocal Microscopy sessions, respectively.

I also want to thank all my friends, old and new, for the tips and tricks they gave me and for all the good moments they provided, inside and outside the lab.

Last, but not least, I'd like to thank my family for all their support and for allowing me to proceed my studies.

Resumo

Além de DNA no núcleo, as células também contêm DNA na mitocôndria (mtDNA). O mtDNA apresenta uma forma circular e codifica 13 proteínas, 2 rRNAs e 22 tRNAs que são exclusivos para este organelo. A mitocôndria tem diversas funções, entre as quais a produção de energia, produzindo a maior parte do ATP usado pelas células via respiração aeróbia.

Durante a respiração celular, ocorre um processo de oxidação/redução produzindo eventualmente ROS, ou espécies reativas de oxigénio, que podem danificar não só a célula e os seus organelos, mas também o mtDNA. Devido à falta de mecanismos de proteção do conteúdo genético, a taxa de mutação do genoma mitocondrial é extremamente elevada quando comparada à taxa de mutação do genoma nuclear.

Sabe-se atualmente que mutações no mtDNA estão ligadas a várias doenças, entre elas a diabetes, cancro, doença de Alzheimer e doença de Parkinson. Nenhuma destas doenças tem um tratamento eficaz, o que incentiva o estudo de novas terapias. A terapia génica, envolvendo a inserção de novos genes em mitocôndrias mutadas com vista a reestabelecer a sua função normal, oferece uma boa perspetiva de tratamento. A terapia génica para mutações mitocondriais ainda se encontra nas fases iniciais de estudo, não tendo ainda sido desenvolvido um método de entrega de material genético, à mitocôndria, suficientemente eficaz e livre de riscos.

Esta dissertação focou-se no desenvolvimento de nanopartículas com afinidade pela mitocôndria para transporte de DNA plasmídico, assim como no desenvolvimento de um vetor incorporando o gene mitocondrial, ND1. O projeto foi dividido em três partes:

1. Isolamento e purificação do gene ND1, biossíntese dos plasmídeos pVAX1-*Lac*Z, pcDNA3-myc-FLNa S2152A e pCAG-GFP e construção do vetor;
2. Produção e caracterização de nanopartículas de DNA plasmídico;
3. Estudos *in vitro*.

O gene mitocondrial ND1, isolado de amostras de sangue humano, foi clonado com sucesso no plasmídeo pGEM®-T. Após a construção do vetor procedeu-se à transformação de *Escherichia coli* através do processo de transformação química. Este passo relevante tornou-se crucial nas etapas subsequentes de desenvolvimento de vetores de expressão com base em genes mitocondriais (investigação em curso).

As nanopartículas foram produzidas usando um método de co-precipitação, produzindo partículas de carbonato de cálcio ($CaCO_3$) incorporando o plasmídeo e rodamina 123, um

composto fluorescente com afinidade mitocondrial. Parâmetros como a morfologia, tamanho, potencial ζ, capacidade de encapsulação e biocompatibilidade foram analisados.

Os resultados demonstraram que as nanopartículas têm características ideais para ensaios de transfeção celular, o que nos permitiu prosseguir com estudos *in vitro* em fibroblastos e células tumorais.

Para avaliar a capacidade de direcionamento e entrega de DNA plasmídico à mitocôndria, procedeu-se à quantificação da proteína GFP expressa. Devido a diferenças no código genético, a proteína GFP não pode ser expressa na mitocôndria quando a transfeção celular é mediada por nanopartículas de pCAG-GFP contendo rodamina 123. A análise à fluorescência da rodamina nas células mostrou também que as nanopartículas se acumulavam na mitocôndria. Estes resultados foram ainda confirmados por microscopia confocal, nomeadamente, por estudos de co-localização a duas e três dimensões.

Assim, nesta dissertação é apresentado um novo vetor não viral com afinidade pela mitocôndria bem como avanços importantes na clonagem de um gene mitocondrial. O conhecimento adquirido, em muito, contribui para a evolução de protocolos de terapia génica mitocondrial motivando a investigação de novos tratamentos para as doenças mitocondriais.

Palavras-chave

Citopatias mitocondriais; Vetores não virais; Terapia génica mitocondrial; Nanopartículas

Abstract

Besides DNA in the nucleus, cells also contain DNA in the mitochondria (mtDNA). This mtDNA encodes for 13 proteins, 2 rRNAs and 22 tRNAs, all exclusive to this organelle. Since their main function is the production of energy, any mutation in the mtDNA can cause serious diseases. The environment inside the mitochondria and the lack of protection of the mtDNA exacerbate the mutation rate of the mitochondrial genome.

Mutations in the mtDNA have already been linked to various pathologies such as diabetes, cancer, Alzheimer's and Parkinson's diseases. Currently, no effective treatment exists for these mitochondrial cytopathies. The development of gene therapy to treat mtDNA disorders offers a promising approach, being a practical and potentially effective tool as it focuses in the actual cause of the disorder.

This M.Sc. thesis focused on the development of a mitochondrial gene based plasmid DNA vector and plasmid DNA nanoparticle systems with the ability to target mitochondria. The project was divided in three main parts:

1. Isolation and purification of ND1 gene and biosynthesis of the plasmids pVAX1-LacZ, pcDNA3-myc-FLNa S2152A and pCAG-GFP and vector construction
2. Nanoparticle formulation and characterization
3. *In vitro* studies

We were able to create a mitochondrial ND1 gene pGEM®-T plasmid vector, opening the way to the formulation of adequate human mitochondrial gene based carriers.

Additionally, we developed novel rhodamine pDNA nanoparticles by a co-precipitation method. These pDNA vectors show a great biocompatibility and suitable size for gene therapy protocols. All rhodamine nanoparticles can be internalized in fibroblast and tumoral cells and target mitochondria. A three-dimensional analysis performed on Z plane confirms the internalization of rhodamine pDNA carriers into mitochondria. In addition, GFP protein inexpression reinforces mitochondrial-targeting ability; due to the different genetic code in mitochondria, GFP protein cannot be expressed.

These results represent a promising new approach to the treatment of mitochondria associated diseases.

Keywords

Mitochondrial cytopathies; Non-viral vectors; Mitochondrial gene therapy; Nanoparticles

Index

Figures List

Tables List

Acronyms Lists

$^{\bullet}OH$ ..... *hydroxyl radical*

Acetyl-CoA ..... *acetyl coenzyme A*

ADA-SCID ..... *adenosine deaminase deficiency*

AP ..... *apurinic/apyrimidinic*

APE ..... *apurinic/apyrimidinic endonuclease*

ATP ..... *adenosine triphosphate*

BER ..... *base excision repair*

$CaCO_3$ ..... *calcium carbonate*

CM ..... *cristae membrane*

cyt *c* ..... *cytochrome c*

DMSO ..... *dimethyl sulfoxide*

DNA ..... *deoxyribonucleic acid*

DQA ..... *dequalinium*

EDTA ..... *ethylenediaminetetraacetic acid*

EE% ..... *encapsulation efficiency*

FDA ..... *US Food and Drug Administration*

FEN ..... *flap endonuclease*

GFP ..... *green fluorescent protein*

GPX ..... *glutathione peroxidase*

H_2O_2 ..... *hydrogen peroxide*

IBM ..... *inner boundary membrane*

IM ..... *inner mitochondrial membrane*

IMS ..... *intermembrane space*

LHON ..... *leber hereditary optic neuropathy*

LIG ..... *DNA ligase*

LP-BER ..... *long patch base excision repair*

MELAS ..... *mitochondrial encephalomyopathy, lactic acidosis, and stroke-like episodes*

MERRF .....*myoclonic epilepsy with ragged red fibers*

mLP.....*mitochondrial leader protein*

mtDNA .....*mitochondrial DNA*

NADH .....*nicotinamide adenine dinucleotide, reduced*

$O_2^{\bullet-}$ ..... *superoxide radical anions*

OM .....*outer mitochondrial membrane*

OXPHOS .....*oxidative phosphorylation*

PBS ..... *phosphate buffered saline buffer*

PCR ..... *polymerase chain reaction*

PEI ..... *poly(ethylenimine)*

PFA ..... *paraformaldehyde*

PLL ..... *poly(L-lysine)*

QH_2 ..... *ubiquinol*

RNA..... *ribonucleic acid*

ROS .....*reactive oxygen species*

rRNA.....*ribosomal RNA*

SCID .....*severe combined immunodeficiency disease*

SN-BER .....*single nucleotide base excision repair*

SOB .....*Super Optimal Broth Medium*

SOD ..... *superoxide dismutase*

TB..... *Terrific Broth Medium*

tRNA..... *transfer RNA*

Chapter 1

Introduction

The human genome, with a DNA sequence of ~6 billion base pairs[1], is organized in 23 chromosomes where, approximately, 21,000 genes, about 1.5% of the entire genome, encode for proteins, and the remaining are non-coding regions, associated with the production of rRNA, tRNA, pseudogenes, and others[2, 3]. Besides the nuclear DNA, there is also DNA inside the mitochondria, called mitochondrial DNA or mtDNA.

Mitochondrial mutations have been linked to various diseases, namely, Parkinson's disease[4], diabetes[5], cancer[6] and others[7, 8]. There are now more than 300 pathogenic mutations described, however, due to the diversity of clinical manifestations, the number may be higher. This diversity is created by the fact that wild-type mitochondria and mutated mitochondria can co-exist in the same cell. It's the ratio of the two types of mitochondria that dictate the severity or the existence of a pathological phenotype, making it difficult to assign a patient to a clinical group. It's estimated that 1 in 200 people have a mutated mtDNA, but due to heteroplasmy, the mixture of mutated and normal mitochondria in the cell, the phenotype may never be manifested[9, 10].

Gene therapy consists in the delivery of an oligonucleotide, DNA or RNA, to a cell in order to treat a certain disease. Currently, cancer gene therapy is one of the most researched, composing more than 60% of all the gene therapy clinical trials[11]. The delivery of these oligonucleotides can involve a myriad of techniques, and can be applied *in vivo* or *ex vivo*. The delivery systems, or vectors, can be either viral or non-viral. The viral vectors, as the name implies, involve the use of modified virus, with the pathogenicity removed or reduced, and have a high transfection rate. However, they have some disadvantages such as the immune response that they can induce. The most commonly used non-viral vectors are lipids, peptides or nanoparticles, and, contrary to viral vectors, produce low to no immune response and can be produced in large scale, but have a lower transfection rate[12].

1. The mitochondria

The mitochondria are widely accepted by the scientific community to originate from a prokaryote, thought to be from the family of α-proteobacteria, which entered in a symbiotic relationship with a proto-eukaryotic cell. This relationship involved the interchange of genes between the cell, turning the mitochondria totally dependent of the host cell[13-15].

These organelles have a diameter of 0.5 to 1.2 μm and a length of, approximately, 2 to 7 μm[16, 17]. These ellipsoid shaped organelles consist of two membranes, the outer membrane (OM) and the inner membrane (IM). In the later one, it is possible to distinguish between an inner boundary membrane (IBM) and a cristae membrane (CM). The IBM is close to the OM, while the CM encapsulates some of the intermembrane space to form the cristae[18, 19].

The IM of the mitochondria is especially important for the oxidative respiration, where all the enzymes for the process can be found. The matrix is where the Kreb's Cycle (or Citric Acid Cycle or Tricarboxylic Acid Cycle) takes place and it's also where we can find multiple copies of the mitochondrial DNA (mtDNA)[17].

1.1 Structure and functions

1.1.1 Energy Production

Eukaryotic cells need a vast amount of energy to function properly. This energy comes, in the vast majority, from the conversion of glucose and other carbohydrates into adenosine triphosphate (ATP). After glycolysis, the main pathway for the metabolism of carbohydrates, pyruvate can be converted to ATP anaerobically or aerobically. The latter is carried in the mitochondria by first converting pyruvate to Acetyl coenzyme A (Acetyl-CoA) that enters the Kreb's Cycle to provide reduced nicotinamide adenine dinucleotide (NADH). These are used in the oxidative phosphorylation (OXPHOS)[17, 20].

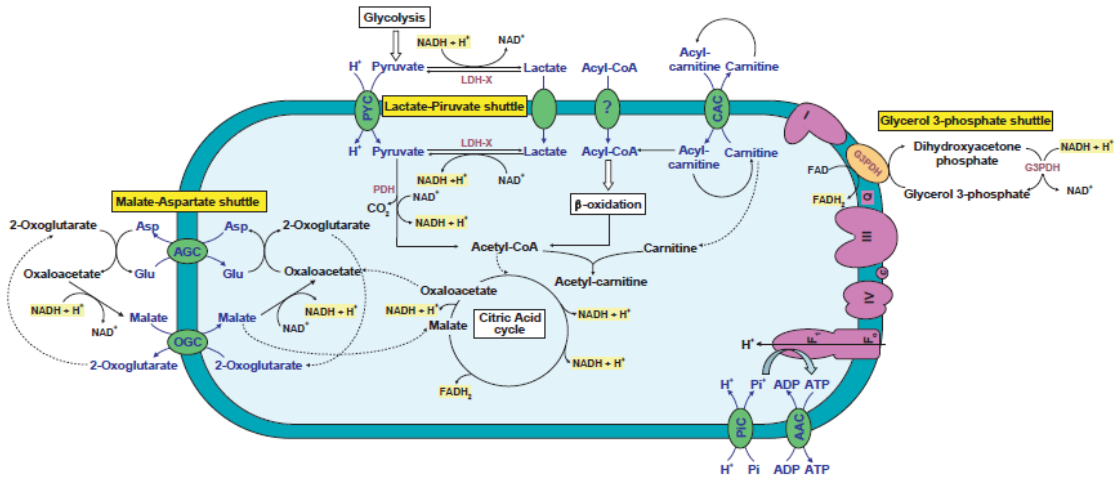

*Figure 1 - **Metabolic pathways present in the mitochondria**. Malate-aspartate, lactate-pyruvate and glycerol 3-phosphate shuttles, Kreb's (or citric acid) cycle, β-oxidation and the electron transportation chain are represented. Adapted from Piomboni et al., 2012[20]*

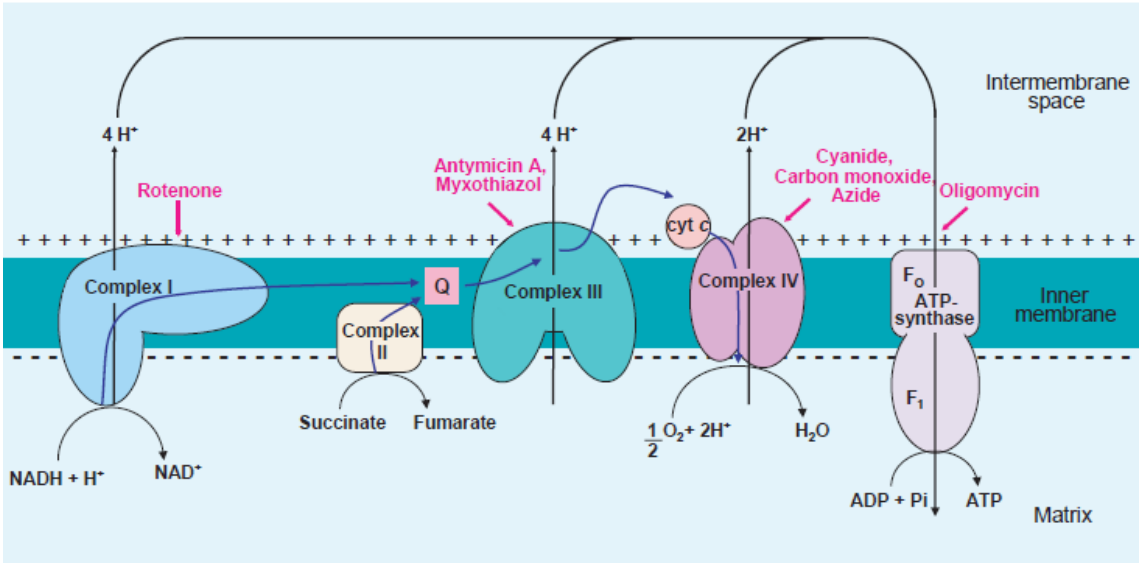

*Figure 2 - **Schematics of the mitochondrial respiratory chain**. In pink, the inhibitors of each complex. Adapted from Piomboni et al., 2012[20]*

The mitochondrial respiratory chain is composed by five multi-subunit complexes, complexes I-IV and ATP synthase, or complex V, and two electron carriers, cytochrome c and ubiquinone, or coenzyme Q (CoQ), and it is responsible for the OXPHOS pathway[20, 21]. Complexes I, III and IV function as proton pumps that increase the proton gradient in the intermembrane space (IMS) and the complex V reduces the gradient generating ATP in the process.

The first step involves the oxidation of NADH, releasing electrons that are transferred to ubiquinone and pumping 4 protons to the IMS. This reaction occurs in Complex I, also called NADH dehydrogenase or NADH:ubiquinone oxidoreductase (E.C. 1.6.5.3.), a large enzyme made of 45 polypeptides, fourteen of them essential for its function and seven of those encoded in the mtDNA (ND1-6 and ND4L). The translated proteins are part of the proton translocation module of the complex.

Ubiquinone can also be reduced via complex II, or succinate dehydrogenase (E.C. 1.3.5.1.), by oxidizing succinate to fumarate. The reduced ubiquinone, or ubiquinol (QH_2), is then reoxidized by complex III, or cytochrome bc_1 complex (E.C. 1.10.2.2), by transferring its electrons to cytochrome *c*, and 4 more protons are released to the IMS.

Cytochrome *c* is oxidized by complex IV, or cytochrome oxidase (E.C. 1.9.3.1.), reducing molecular oxygen to H_2O and pumping 2 more protons. Since the IM is impermeable to protons, these can only re-enter the matrix through a pump, in this case, ATP synthase or complex V (E.C. 3.6.3.14.). The existence of a proton gradient drives the synthesis of ATP[21-23].

1.1.2 ROS Production and Regulation

During the OXPHOS, some electrons can escape and react with O_2, reducing it to $O_2^{\bullet-}$. This occurs mainly in complexes I and III, but recent studies also suggest that complex II may be involved[24]. Reactive Oxygen Species, or ROS, are reactive molecules and radicals derived from oxygen that can oxidize other molecules. $O_2^{\bullet-}$ can be neutralized in the mitochondrial matrix, by superoxide dismutase-2 (SOD2 or Mn-SOD), or in the cytoplasm, by superoxide dismutase-1 (SOD1 or Cu/Zn-SOD), forming hydrogen peroxide (H_2O_2).

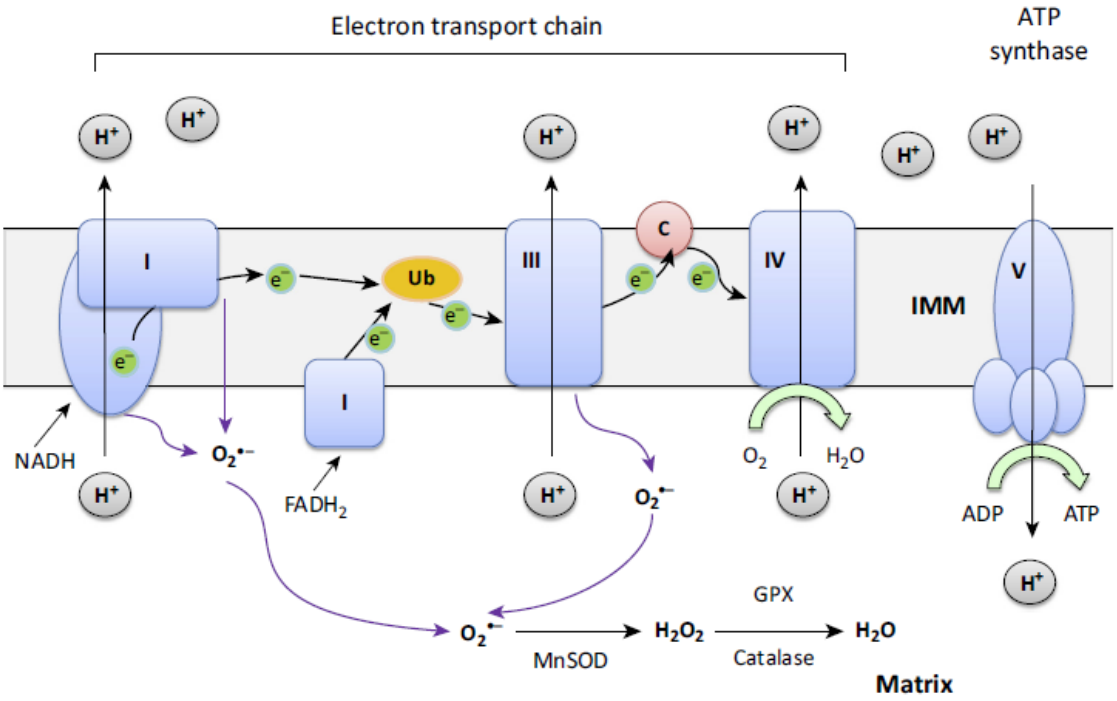

*Figure 3 - **Production of ROS in the mitochondrial respiratory chain**. Some electrons can escape the electron transport chain and produce $O_2^{\bullet-}$. In the matrix, manganese superoxide dismutase (Mn-SOD) converts it to H_2O_2 that can then be reduced to H_2O by either catalase or glutathione peroxidase (GPX). Adapted from Yu et al., 2014[25]*

H_2O_2 is usually converted to H_2O by catalase or glutathione peroxidase (GPX). However, in the presence of Fe^{2+} or Cu^{+}, H_2O_2 can create the $^{\bullet}OH$ radical, a highly reactive radical with a very short half-life, approximately 10^{-9} s.

ROS can interact with lipids, degrading the cellular membranes in a process called lipid peroxidation, with proteins, altering their structure, and therefore their function, and can also damage DNA, either by degrading it or modifying the nucleic bases[26-29].

1.1.3 Calcium Homeostasis

Calcium ions, Ca^{2+}, are used in the cell in various signalling pathways and are able to bond to thousands of proteins, changing their conformation and function[30].

Increase of Ca^{2+} inside the mitochondria increases the activity of many enzymes involved in the Kreb's Cycle and OXPHOS, leading to the increase of production of ATP. However, Ca^{2+} overload can cause necrosis of the tissue, by the collapse of the membrane potential and swelling of the mitochondria[31, 32].

Apoptosis, or programed cell death, can also be triggered by the influx of Ca^{2+}. Calcium will induce the release of cytochrome *c* (cyt *c*), that will activate the caspase cascade leading to the cell's death[33].

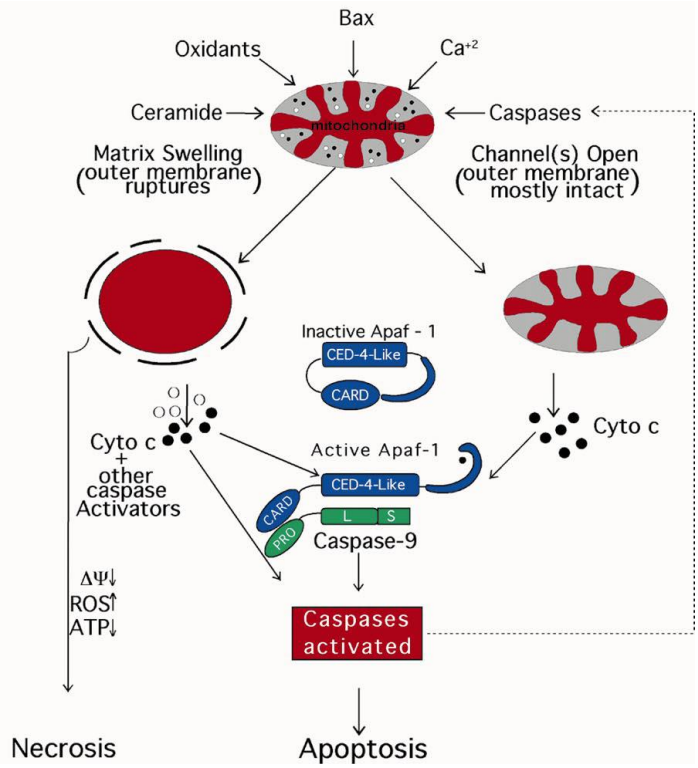

*Figure 4 - **Metabolic pathways leading to apoptosis and necrosis**. Outside stimuli can lead to the mitochondrial swelling, rupturing the membrane and release of cyt-c triggering apoptosis. Necrosis can also occur due to the release of ROS (left). If the membrane channels open, the organelle remains intact, releasing only cyt c, activating the caspase cascade, leading to apoptosis. Adapted from Green et al., 1998[34]*

1.1.4 Immunological Responses

Mitochondria have been linked to the innate immunity by interacting with the pathways associated with the defence against foreign organisms. This happens primarily if the mitochondria are damaged, either by a virus or during necrosis, releasing their components in the cytosol. Due to the bacterial nature of the organelle, the cell will recognise these molecules as foreign and possibly dangerous, triggering an immune response[35-37].

1.2 The mitochondrial DNA

1.2.1 Structure and Inheritance Mechanisms

The mitochondrial DNA is a circular, double stranded molecule with approximately 16 kbp, and contains 37 genes, encoding 13 proteins that take part in the oxidative phosphorylation chain, 2 rRNAs and 22 tRNAs, all exclusive to the mitochondria. Mutations in any of these genes could cause serious problems to tissues that contain a high level of these organelles, like the heart or the brain. However, due to the self-replicating and self-expressing nature of the mitochondria, the presence and severity of the disease is highly dependent of the number of mitochondria affected by the mutation[38-40]. The existence of varying numbers of diseased and wild-type mitochondria in the cell is called heteroplasmy. Homoplasmy occurs when the cell only contains normal or diseased mitochondria, the latter one being, in some cases, incompatible with life[7, 19].

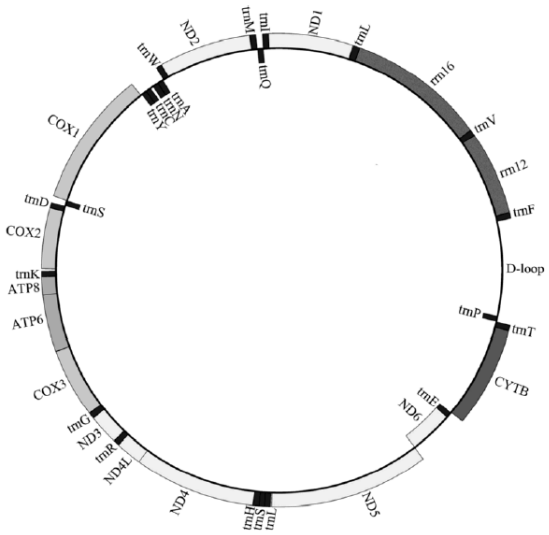

*Figure 5 - **Map of mtDNA**. Adapted from Tao et al.[41]*

Transmission of these mutations does not follow a Mendelian inheritance. During oogenesis, mitochondria are segregated randomly to daughter cells, resulting in some cells having few mutated mitochondria and other having few wild type mitochondria. Heteroplasmy does not necessarily mean that the individual will have a clinical phenotype. It appears that each mutation type has a different threshold, in other words, different levels of heteroplasmy are needed for a disease to manifest[42, 43].

Paternal inheritance of mitochondria has only been observed once in humans[44], although in other mammals it's very common[45]. This appears to be caused by the ubiquitination of the spermatozoa mitochondria, and subsequent degradation in the oocyte after fertilization[46].

1.2.2 Mutations and Repair Mechanisms

Mutations in the mtDNA occur primarily due to damage caused by ROS produced during OXPHOS. ROS react with free nucleotides in various ways, either by attacking the sugar backbone or the nitrogenous base. These can also be caused by natural oxidants present in the cell or exposed to the organism, and can be aggravated since some of the products of the reactions are more easily oxidized, creating even more mutated nucleotides.

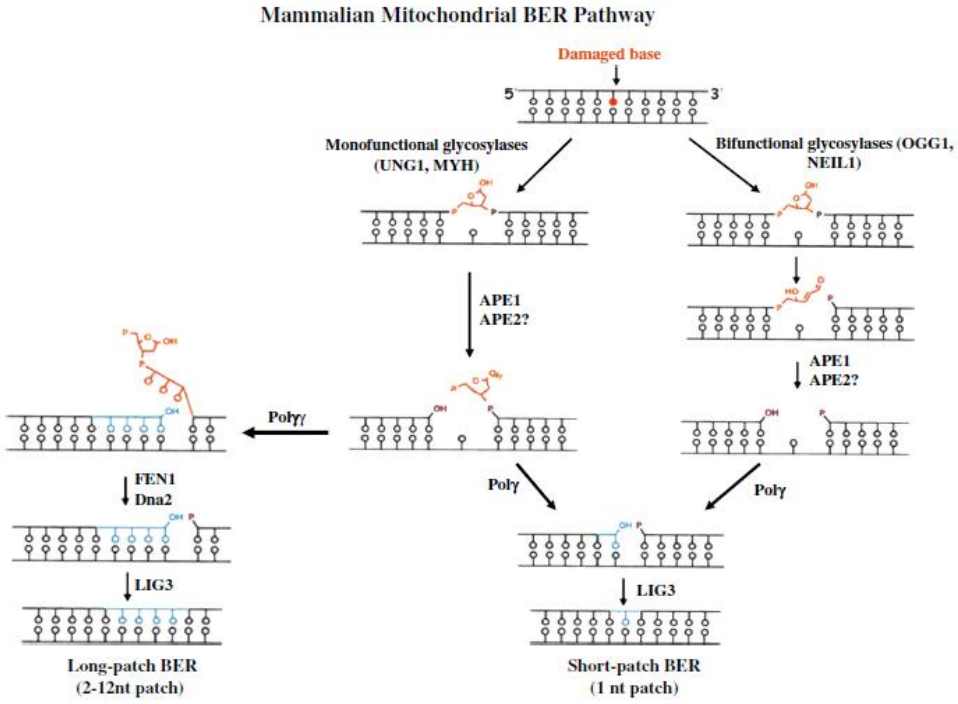

*Figure 6 - **Base excision repair mechanism in mammalian mitochondria**.*[47]

Although the mutation rate of the mtDNA is high, the mitochondria possesses repair mechanisms to recover the normal sequence. Currently, several repair pathways have been described; the primary ones are the single-nucleotide base excision repair (SN-BER) and the long-patch BER (LP-BER).

Base excision repair (BER) can be divided in two sub-pathways, short-patch BER, where only one nucleotide is repaired, and long-patch BER, with two to twelve nucleotides repaired. Both occur in four steps. The first step involves the recognition by a DNA glycosylate of a mutated base, removing the nitrous base and creating an abasic site (or apurinic/apyrimidinic site, or AP site). This site is then recognised by an AP endonuclease (APE1) that removes the AP site or simply opens the strand of DNA. DNA polymerase adds the missing nucleotide, or nucleotides, to the strand and, in some cases, leaving a piece of DNA, called 5' flap, still connected that contains the AP site. This is removed by the Flap endonuclease (FEN1), allowing the conclusion of the process by DNA ligase III (LIG3) that connects all the nicks between nucleotides[47, 48].

1.2.2.1 Ageing

It is well established that the production of ROS in the mitochondria can lead to an accumulation of mtDNA mutations, which can lead to cell dysfunction and possibly death. However, the connection of abnormal mitochondrial function and ageing has not been clearly defined. Some of the hypothesis involve the accumulation of mtDNA mutation, others the increase of production of ROS, and others the individual's diet, but all of them have been insufficient explanations for a conclusive statement in this subject. Nonetheless, the proper functioning of mitochondria seems to be important to delay the effects of ageing[49, 50].

1.2.2.2 Mitochondrial Associated Diseases

Being the main source of energy in the cells, any alteration on the function of mitochondria can cause serious problems in high energy demanding tissues like the heart or the brain. Many mutations in mtDNA have been described, most of them being point mutations in genes encoding Complex I proteins and tRNAs[51]. The most common tRNA mutation occurs in $tRNA^{Leu(UUR)}$ and $tRNA^{Lys}$, and are associated with Mitochondrial Encephalomyopathy, Lactic Acidosis, and Stroke-like episodes (MELAS) and Myoclonic Epilepsy with Ragged Red Fibres (MERRF) syndrome respectively[52].

MELAS (MIM: 540000) is characterized mainly by stroke-like episodes, seizures, mental retardation, muscle weakness and short stature[53, 54]. It was first described by Pavlakis et al. in 1984[55] and Goto et al. discovered a mutation in mtDNA, m.3243A>G in the $tRNA^{Leu(UUR)}$ gene, present in 80% of the patients with the disease[56]. Mutations related to this disease were also found in $tRNA^{Gln}$, $tRNA^{His}$, $tRNA^{Lys}$, $tRNA^{Cys}$, $tRNA^{Ser(UCN)}$, $tRNA^{Ser(AGY)}$, ND1, ND5 and ND6, all genes present in the mitochondrial genome[57].

MERRF (MIM: 545000) has similar symptoms to MELAS, namely the short stature, seizures and dementia, but one of the distinctive characteristics is the accumulation of mitochondria in the muscle fibres, giving them the appearance of red-ragged fibres[54]. It was first reported by Fukuhara et al. in 1980[58], and 80% of the cases present a mutation, m.8344A>G, in $tRNA^{Lys}$, as described by Shoffner et al.[59]. Other mutations were also discovered in $tRNA^{Leu(UUR)}$, $tRNA^{His}$, $tRNA^{Ser(UCN)}$, $tRNA^{Ser(AGY)}$ and $tRNA^{Phe}$ [57].

Complex I mutations, involving the mitochondrial ND genes, are also present in individuals with Leber Hereditary Optic Neuropathy (LHON) (MIM: 535000), one of the most common mitochondria-related diseases. It was first described by Theodor Leber in 1871[60] and leaves patients with acute vision loss and the mutations tend to be homoplasmic[54].

The genes affected are usually the ND1 (m.3460G>A, 60%-80% of the cases), ND4 (m.11778G>A, 0%-50%) and ND6 (m.14484T>C, 0%-65%), between others, but these genes alone can also cause other disorders, as previously mentioned[10, 43, 57]. ND1 has also been associated with Parkinson's disease, although it's not a primary cause of the disorder[61, 62].

2. Gene Therapy

Gene therapy can be defined as the delivery of a nucleic acid, RNA or DNA, in a target cell or tissue with a therapeutic end. This method can be applied either in somatic or germ line cells, but only the former one is currently approved for use in humans. Germ line cells gene therapy is avoided due to the possibility of transferring the genetic changes to the offspring, potentially causing undesirable effects.

The first step towards a genetic therapy is to identify a gene that, when mutated, causes a disease. When the gene is identified, researchers construct a vector that contains a copy of the gene in its functional form. The vector can then be delivered to the affected tissue using a myriad of techniques, ranging from electroporation, biobalistics and ultrasounds, called physical methods, to the use of delivery systems based on complexes made from lipids or inorganic compounds, called chemical methods, or even using viruses.

This approach presents many advantages when compared to "conventional" therapeutics. The treatments that are now used in the diverse diseases consist in supplying the patient with drugs or proteins, for example insulin. The main disadvantages are the costs of the production of such treatments and the fact that the patient has to take these compounds for a long time, or even for life. Proteins also have the possibility of being filtered in the blood by the kidneys or be degraded before reaching their target, reducing their overall bioavailability. Another drawback of the current medicines is the toxicity associated, that can be aggravated if many doses need to be applied.

Gene therapy circumvents some of these problems since it tries to solve the problem in the actual cause of the disorder. The quantities of protein are controlled by the cell itself, reducing the possibility of toxic effects and the treatment also lasts longer, reducing, or even eliminating, the need for new protein injections. However, the delivery of these genes is not yet as efficient as desired, the cell can create an immune response to the foreign nucleic acid, and, if the delivery method is of viral nature, the gene can integrate in the genome at a random place causing alterations in the expression of DNA[63].

The first human trial started in 1990, after approval by the FDA, in two patients with severe combined immunodeficiency disease due to adenosine deaminase deficiency (ADA-SCID). One of the patients, Ashanti DeSilva, had a significant response to the treatment, opening the way to new clinical trials[11, 64]. As of June 2014, 2,076 clinical trials, in all phases, were running, 75 of them in phase III and 2 in phase IV (http://www.abedia.com/wiley/phases.php). In 2012, the European Medicines Agency recommended approval of the first gene therapy product, Glybera, for patients with lipoprotein lipase deficiency.

2.1 Viral and Non-viral Gene Therapy

Two different approaches can be considered for gene delivery: viral and non-viral. The first uses a modified virus, taking advantage of their natural ability of transferring DNA or RNA into the host cell. The nucleic acid inside the virus' capsid is manipulated to remove the genes that confer pathogenicity and the genes that allow the replication inside the cell. There are some drawbacks, since the host's immune system can react to the virus causing an immune response, reducing future treatments efficiency[65].

The viruses used can be of four types, adenovirus, adeno-associated virus, lentivirus and retrovirus. All of them have the general disadvantage of this approach in relation to the non-viral approach, that is, the small packaging capacity of DNA/RNA (~8 kb). The lentivirus and retrovirus have also the ability to integrate their genetic information with the host's DNA[12, 66].

Non-viral gene therapy methods have been extensively studied lately due to the advantages they present. They are safer, cheaper, less toxic, and thus have a higher biocompatibility, and can carry larger genes, theoretically with limitless size. However, the transfection efficiency is lower than using viral methods. Widely used compounds are cationic lipids or cationic polymers that form lipoplexes or polyplexes, respectively, by interacting with plasmid DNA. This is achieved due to the positive charge that the lipids and the polymers have at physiological pH, allowing the encapsulation of pDNA due to is negative charge. The complexes are internalized in the cell by endocytosis, releasing the contents in the cytosol. Cationic lipids consist in a hydrophilic and a hydrophobic group, and a linker that connects both groups. Depending on the chemical composition, three groups can be defined: hydrocarbon chain, cholesterol or vitamin D based lipids. Cationic polymers are primarily amine based and can be tailored to obtain the best properties for the intended use. They can be divided in various groups, but the most studied are the poly(ethylenimine) (PEI), poly(L-lysine) (PLL) and chitosan based polymers[67, 68].

Lipoplexes and polyplexes still have an inherent toxicity and low transfection efficiency, giving rise to the need of a new carrier. Thus, researchers began to study inorganic alternatives. One of the most widely used methods is the calcium phosphate (CaP) co-precipitation technique, however the characteristics and transfection conditions of the co-precipitates are hard to control[69]. These problems were circumvented by utilizing calcium carbonate ($CaCO_3$) having high biocompatibility and being able to dissociate inside the cell, thus releasing its components[70, 71].

2.2 Mitochondrial Gene Therapy

All the previously referred methods are used to deliver genetic information to the nucleus, but in order to correct mitochondrial associated diseases, we need to target the mitochondria

and transverse its barriers. One way is to use the protein import pathway of the mitochondria. Mitochondrial leader proteins (mLP) have been used to allow the entry of DNA into the organelle by linking them together and transfecting them in the cell using a liposome.

D'Souza and co-workers have been studying the use of dequalinium (DQA), a lipophilic compound with a double positive charge that accumulates in the mitochondria[72], to create what they call DQAsomes, a system capable of entering the cell and with high affinity to the mitochondria[39]. Their studies show the ability of these compounds of delivering nucleic acids to the mitochondria[73-75]. The earlier formulations were, however, highly toxic to mammalian cells[76], and since then improvements were made to circumvent the problem[39, 77].

Yu and co-workers used a viral approach to the treatment of mtDNA mutations. They used a modified Adeno-Associated Virus (AAV) capsid, containing a mitochondrial protein fused to one of its own proteins, and inserted a ND4 encoding plasmid. The viruses where used in cultured cells and in mice, where they verified the expression of ND4 during several months[78, 79].

Other approach was tested by Yamada and co-workers which have developed a liposome-based carrier, called MITO-porter, capable of delivering bioactive compounds and macromolecules including pDNA. This carrier fuses with the OM, delivering its contents in the mitochondrial matrix[80-84].

The usage of inorganic nanoparticles has not been widely studied when it comes to mitochondrial gene therapy, but our group has been able to develop a promising new carrier, using the $CaCO_3$ method, capable of targeting the mitochondria when incorporating rhodamine 123, a probe with high affinity to the mitochondria[85]. This thesis pretends to continue the previous work in order to demonstrate, mainly through in vitro studies, the mitochondrial targeting ability of these carriers and to develop a new plasmid vector containing the ND1 mitochondrial gene.

2.3 Vector Construction and Amplification

One of the most important aspects of gene therapy is the design of a vector containing the gene of interest to be expressed in the right organelle. The plasmid must be easily produced, must have an antibiotic resistance gene in order to effectively select the transformed cells during production and must have restriction sites that allow the insertion of the gene. Amplification of the vector is usually made using transformed *E. coli*, allowing them to grow in a media rich in nutrients.

2.3.1 Mitochondrial DNA Amplification challenges

Amplification of mtDNA has been extremely difficult, especially human mtDNA. Rat mtDNA has already been amplified in *E. coli* in its entirety[86, 87]. Coutelle and co-workers were able to clone the complete human mtDNA in *Saccharomyces cerevisiae*, but were unable to clone it in *E. coli*, proposing that the tRNA genes and the D-loop may be the cause of failure[88].

In this thesis, we tried to create, for the first time, a ND1 mitochondrial gene based vector for the development of gene therapy protocols as a new perspective for the treatment of mitochondrial DNA disorders. This particular gene has been associated with various diseases, LHON, MELAS and Parkinson's. ND1 encodes for a subunit of Complex I of the OXPHOS, the main energy producing pathway.

Chapter 2

Materials and Methods

1. Materials

1.1 Reagents

Dulbecco's Modified Eagle Medium (DMEM) and Dulbecco's Modified Eagle Medium Nutrient Mixture F12 (DMEM F-12) were obtained from Biochrom AG (Germany). Tween 20 and Triton X-100 were obtained from Fisher Scientific (Waltham, Massachusetts, USA). Paraformaldehyde (PFA) and Trypan Blue were obtained from Merk (Whitehouse Station, New Jersey, United States). LB broth was obtained from Liofilchem (Roseto degli Abruzzi, Italy) and LB-Agar was obtained from Pronadisa/Conda (Madrid, Sapin). Yeast Extract was obtained from Himedia (Mumbai, India) and Tryptone was obtained from Biokar (France). Glycerol and $CaCl_2$ were obtained from VWR International (Radnor, PA, USA). KH_2PO_4 was obtained from Chem-Lab (Zedelgem, Belgium) and Na_2CO_3 and K_2HPO_4 were obtained from Panreac (Barcelona, Spain). Agarose and Green Safe were obtained from NZYTech (Lisboa, Portugal). Cellulose was obtained from Aldrich Chemical Company (Milwaukee, WI, USA). Hoechst 33342 (trihydrochloride, trihydrate) was obtained from Invitrogen (Carlsbad, CA) while Mito Tracker Orange CMTMRos is from Molecular Probes (Oregon, USA). Rhodamine 123 was obtained from Sigma-Aldrich (St. Louis, MO, USA). Normal Human Dermal Fibroblast (NHDF) adult donor cells were purchased from PromoCell (Heidelberg, Germany), cancer HeLa cells from ATCC (Middlesex, UK) and mouse brain neuroblastoma cells (N2a) from Invitrogen.

1.2 Plasmids

pVAX1-*LacZ* was obtained from Invitrogen (Carlsband, CA, USA) while both pcDNA3-myc-*FLNa* S2152A, plasmid 8983, and pCAG-GFP, plasmid 11150, were obtained from Addgene (Cambridge, MA, USA).

2. Methods

2.1 Competent Cell Preparation

To prepare competent cells, an adapted version of Inoue's protocol[89] was used. One colony, from a previously inoculated plate, was transferred to 25 mL of Super Optimal Broth (SOB) medium (0.5% (w/v) yeast extract, 2% (w/v) tryptone, 10 mM NaCl, 2.5 mM KCl, 20 mM $MgSO_4$) and incubated for 6 to 8 hours at 37 ºC and 250 rpm. 10 mL, 4 mL and 2 mL of this culture was then distributed to three 1 L Erlenmeyer flasks with 250 mL of SOB medium and incubated overnight at 18 ºC and 250 rpm. Once one of the cultures reached 0.55 of OD_{600}, the growth was stopped by transferring the flask to a cold water bath for 10 min. The remaining cultures were discarded.

The cells were harvested by centrifuging for 10 min at 4 ºC and 2,500 x *g* and resuspended in 80 mL of ice-cold Inoue Transformation Buffer (ITB) buffer ($MnCl_2.4H_2O$ 55 mM, $CaCl_2.2H_2O$ 15 mM, KCl 250 mM, PIPES 10 mM) and centrifuged again. Finally, the cells were resuspended in 20 mL of ice-cold ITB buffer with 1.5 mL of dimethyl sulfoxide (DMSO) and incubated for 10 min in ice. Aliquots were made by freezing the cells first in liquid nitrogen and then stored at -80 ºC.

Cell competence was evaluated by transforming the cells with 50 ng of pDNA using heat shock. The colonies were observed after incubation at 37 ºC overnight and counted to calculate the transformation efficiency. The formula used was the following:

$$\%TE = \frac{Dilution\ Factor \times number\ of\ colonies}{\mu g\ of\ pDNA\ used} \quad (1)$$

2.2 Plasmids amplification and purification

The pCAG-GFP, pVAX1-*LacZ* and pcDNA3-myc-*FLNa* S2152A plasmids were produced by fermentation with *E. coli* JM109 cell in 125 mL of Terrific Broth (TB) Medium (20 g/L tryptone, 24 g/L yeast extract, 4 mL/L glycerol, 0.017 M KH_2PO_4, 0.072 M K_2HPO_4) in 500 mL Erlenmeyers. The fermentation was carried in the presence of 100 µg/mL of ampicillin with 30 µg/mL of nalidixic acid for the cells transformed with pCAG-GFP, 30 µg/mL of kanamycin for the cells transformed with pVAX1-*LacZ* and 100 µg/mL of ampicillin with 100 µg/mL of neomycin for the cells transformed with pcDNA3-myc-*FLNa* S2152A.

Fermentation was carried overnight at 37 ºC and 250 rpm. At OD_{600} ≈ 7-9 (late log phase), the cells were harvested by centrifugation at 4 ºC and 4,500 rpm for 10 min in an Allegra 25R centrifuge (Beckman Coulter, CA, USA).

Purification of the plasmid was accomplished using QIAGEN® Plasmid Purification kit. The previously harvested cells were lysed and centrifuged twice at 4 ºC and 20,000 x *g*, first for 30 min and after for 15 min. The supernatant was loaded in a QIAGEN-tip and the contaminants

removed. The pDNA was eluted and precipitated with isopropanol. The solution was centrifuged at 4 ºC and 16,000 x *g* for 30 min and the pellet was resuspended with 70% ethanol and centrifuged again at 4 ºC and 16,000 for 10 min. The pellet, containing the pDNA, was resuspended in 1 mL of TE buffer (10 mM Tris-Cl, 1 mM EDTA, pH 8.0) and the concentration determined by UV spectrophotometry at 260 nm. The pDNA was aliquoted in 1 mL aliquots with a concentration of 100 µg/mL of pDNA.

2.3 Plasmid Sequencing

The pCAG-GFP plasmid, obtained from the fermentation, was sequenced by adapting the Beckman Coulter's GenomeLab™ Dye Terminator Cycle Sequencing protocol. We were only interested in sequencing this plasmid since the vector that we proposed to construct used pCAG-GFP, due to the existence of the expression marker Green Fluorescent Protein (GFP). This sequencing step allowed us to verify that the plasmid obtained during the fermentation was pCAG-GFP.

In short, approximately 50 fmol of purified plasmid were mixed with 0.25 µL of 0.25 µM primer (RV: EGFP-N CGTCGCCGTCCAGCTCGACCAG), 4 µL of DTCS Quick Start Master Mix and ddH_2O to a final volume of 10 µL. The thermal cycling program used is displayed in table 2 and conducted in a T100™ Thermal Cycler (Bio-Rad, CA, USA):

Table 1 - Thermal cycle used during sequencing.

TEMP. (ºC)	TIME	
98	5min	
96	20sec	x30
50	20sec	
60	4min	
60	10min	
4	Until usage	

To each reaction tube, 3 µL of Stop Solution/Glycogen mixture (1.2 µL of 3 M Sodium Acetate, pH 5.3, 1.2 µL of 100 mM Na_2-EDTA, pH 8.0, and 0.6 µL of 20 mg/mL of glycogen) and 60 µL of chilled 95%(v/v) ethanol was added. Centrifugation was carried at 3,000 rpm for 30 min. The obtained pellet was washed two times with chilled 70%(v/v) ethanol, centrifuging at 3,000 rpm for 5 min between each step. After dried, the pellet was resuspended in 10 µL of Sample Loading Solution.

Plasmid sequencing was carried with a GenomeLab™ GeXP Genetic Analysis System (Beckman Coulter, California, USA).

2.4 ND1 gene amplification and vector construction

Human mitochondrial DNA was extracted from blood samples, and the ND1 gene was amplified by polymerase chain reaction (PCR) using mtDNA as template and the following primers: FW: GCAGAGCCCGGTAATCGCATA and RV: GGATTCTCAGGGATGGGTTC. The PCR reaction occurred in a final volume of 15µL containing 1 U DreamTaq™ Green DNA polymerase (Fermentas, MA, USA), 2 mM $MgCl_2$, 0.2 mM dNTPs, 0.25 mM of each primer and 100-300 ng of mtDNA. This reaction was conducted in a T100™ Thermal Cycler (Bio-Rad, CA, USA). The PCR product was purified using the GRS PCR & Gel Band Purification Kit (GRiSP, Porto, Portugal).

Table 2 - Thermal cycle used during ND1 amplification

TEMP. (°C)	TIME	
95	10 min	
95	30 sec	X40
60	30 sec	
72	30 sec	
72	10 min	
15	Until usage	

Ligation of the ND1 gene to pCAG-GFP, previously digested, was performed, but it was not successfully achieved. We then tried to perform the ligation with pGEM®-T plasmid using the pGEM®-T Vector system kit from Promega (Madison, WI, USA). In short, pDNA and ND1 gene fragments in a 2:1 ratio were added to 5 µL of 2X Rapid Ligation Buffer and 1 µL of T4 ligase and ddH_2O was added to a final volume of 10 µL. The reaction took place at room temperature for at least 1h.

2.5 Agarose gel electrophoresis

Agarose gel electrophoresis was performed to evaluate the size and conformation of the purified pCAG-GFP plasmid and to evaluate the size of the purified gene and the ligation product.

The electrophoresis, a technique that allows the separation of nucleic acid molecules by applying an electric field in an agarose gel matrix, was carried out using a gel with 1% agarose and 1 µg/mL Green Safe and the run occurred at 150 V for 30 min in TAE buffer (40 mM Tris base, 20 mM acetic acid and 1 mM EDTA pH 8.0). The visualization of the gel was made under UV light in an UVItec Gel documentation system (UVItec Limited, Cambridge, United Kingdom).

2.6 ND1 Gene and Designed Vector sequencing

The ND1 gene, obtained from human mtDNA, and the ligation product pGEM®-T-mtND1 were sequenced by adapting the Beckman Coulter's GenomeLab™ Dye Terminator Cycle Sequencing

protocol, as described in 2.4. The primers used were T7 TAATACGACTCACTATAGGG and SP6 TATTTAGGTGACACTATAG for pGEM®-T-mtND1 and FW: GCAGAGCCCGGTAATCGCATA and RV: GGATTCTCAGGGATGGGTTC for mtND1 gene. The primers used for the ligation product allowed us to verify the existence of an insert in pGEM®-T. mtND1 was sequenced to verify that we obtained the gene of interest.

2.7 Nanoparticle Synthesis

The nanoparticles were produced from a solution of $CaCl_2$ at 30 mg/mL and $NaCO_3$ at 42.5 ng/mL. For both systems two solutions were prepared named Solution A and Solution B. Solution A contained 10 µg of pDNA, 120 µL of $CaCl_2$ and, for the synthesis of $CaCO_3$-pDNA-Rho123, 15 µL of Rhodamine 123 and ddH_2O until a final volume of 290 µL. Solution B contained 255 µL of $NaCO_3$ and 5 µL of cellulose at 1 mg/mL. Solution A was added to Solution B dropwise and the final solution was centrifuged at 10,000 rpm for 15 min. The pellet that was formed contained the nanoparticles[71].

2.8 Nanoparticle Characterization

2.8.1 Morphology, size and ζ potential

The nanoparticles in the pellet were washed with ddH_2O trice, centrifuging at 13,000 rpm for 10 min between each washing step, and then resuspended in 20 µL of ddH_2O and 20 µL of 1% (w/v) tungsten. 20 µL were placed in a round coverslip and left to dry at room temperature overnight.

The coverslip was coated with gold using an Emitech K550 sputter coater (London, England) and analysed by scanning electron microscope (SEM) (Hitachi S-3400N, Tokyo, Japan), operated at an accelerating voltage of 20 kV with variable magnifications.

The average particle size of the nanoparticles and the surface charges (zeta potential) were carried out, at 25 ºC, in a Zetasizer nano ZS instrument using a zeta dip cell. Dynamic light scattering using a He-Ne laser 633 nm with non-invasive backscatter optics (NIBS) and electrophoretic light scattering using a patented laser interferometric technique named M3-PALS (Phase analysis Light Scattering) were applied for particle size and zeta potential determination, respectively. The Malvern zetasizer software v6.34 was used. The average values of size and zeta potential were calculated with the data obtained from three measurements ± SD.

2.8.2 Encapsulation Efficiency

To determine the encapsulation efficiency of pDNA, the nanoparticles were prepared as described in 2.7 and the supernatant was recovered. This supernatant contained the unbound pDNA. The analysis was performed in a NanophotometerTM (Implen, Germany) at 260 nm. Triplicates were obtained and ddH_2O was used as the blank experiment. The encapsulation efficiency (EE%) was calculated using the equation:

$$EE\% = \frac{pDNA_{total} + pDNA_{unbound}}{pDNA_{total}} \times 100 \quad (2)$$

2.8.3 Cell Cytotoxicity

Plasmid DNA nanoparticles were applied to a 96-well plate. Before cell seeding, the plates were ultraviolet irradiated for 30 minutes. Human fibroblast cells were plated at a density of $1x10^4$ cells per well in 96 well plate at 37 ºC in 5% CO_2 humidified atmosphere, for 24 and 48 hours. After incubation, the redox activity was assessed through the reduction of the MTT. 100 µL of MTT dye solution (0.05 mg/mL in Krebs) was added to each well, followed by incubation for 2 hours at 37 ºC, in a 5% CO_2 atmosphere. The medium was aspirated and cells were treated with 50 µL of isopropanol/HCl (0.04 N) for 30 minutes. Absorbance at 570 nm was measured using a Biorad Microplate Reader Benchmark. The spectrophotometer was calibrated to zero absorbance using culture medium without cells. The relative cell viability (RCV%) related to control wells was calculated by the following equation:

$$RCV\% = \frac{[A]_{test}}{[A]_{control}} \times 100 \quad (3)$$

$[A]_{test}$ is the absorbance of the test sample and $[A]_{control}$ is the absorbance of control sample. All the experiments were repeated three times in triplicate. The statistical analysis of experimental data used the Student's t-test and the results were presented as mean ± standard deviation. Statistical significance was accepted at a level of $p < 0.05$.

2.9 Cell Lines Culture

Previously frozen HeLa, N2a and Fibroblast cells were thawed at room temperature. The vials' contents were diluted in 5 mL of appropriate medium, DMEM for N2a and DMEM F-12 for HeLa and fibroblasts, and centrifuged at 300 x *g* for 3 min to remove any traces of DMSO. The supernatant was removed and the pellet, containing the cells, was resuspended in 5mL of appropriate medium. The media were then transferred to 25 cm^2 T-Flask and placed in an incubator at 37 ºC and 5% CO_2. Media was changed every two days, when it changed from a pink-red colour to an orange or yellow colour. The medium of HeLa cells was traded for DMEM after the first passage.

The cells were passed ensuring that the confluence never reached levels above 80%/90%. The media were removed from the T-Flasks and the cells were rinsed with pre-warmed PBS (NaCl 8 g/L, KCl 0.2 g/L, $Na_2HPO_4 \cdot 2H_2O$ 1.8 g/L, KH_2PO_4 0.3 g/L with a pH of 7.4). Approximately 2 mL of pre-warmed trypsin was added to the cells and incubated for 2-3 min to ensure the detachment of all the cells. To stop the reaction, 5 mL of appropriate medium was added and the cells transferred to sterile falcon tubes to be centrifuged at 150 x *g* for 5 min. The supernatant was discarded and the cells resuspended in pre-warmed media. From this, 0.5 mL was seeded in new T-Flasks, with 5 mL of fresh media, or used for experiments.

To count the number of cells, 20 µL of the resuspended cells was mixed with 20 µL of Trypan Blue and the count was performed in a Newbauer Chamber. The total number of cells was calculated using the following formula:

$$Cells_{Total} = Cells_{counted} \times 10^5 \quad (4)$$

2.10 Transfection Studies

2.10.1 Cell-associated Rhodamine Fluorescence

After transfection (4 h, 8 h, 12 h, 24 h or 48 h), fibroblasts, HeLa and neuroblastoma cells were washed three times with PBS and vigorously pipetted to facilitate cell detachment. The rhodamine fluorescence intensity was measured using a microplate reader using 485 and 528 nm as excitation and emission wavelengths, respectively. Rhodamine content of each well was determined by using the bicinchoninic acid (BCA) method, following the manufacturer´s protocol (Pierce).

2.10.2 GFP Quantification

After *in vitro* transfection with pCAG-GFP based rhodamine nanoparticles or pCAG-GFP nanoparticles without rhodamine (at least, n = 3), studies proceeded with the quantification of GFP protein by GFP ELISA kit (MitoSciences, ab 117992, Abcam, United Kingdom). This GFP ELISA Kit is an enzyme immunoassay developed for the sensitive detection and quantitation of GFP or GFP fusion proteins in cells or tissue samples. Transfected cell lysates were prepared from detergent lysis (lysis buffer-tissue, 50:50 vol/vol) in lysis buffer (1% Triton X-100 and 0.1% SDS in PBS, pH 7.4 and proteinase inhibitor cocktail) and homogenization. The assay employs a specific GFP antibody coated onto a well plate strips. Standards and samples are pipetted into the wells and GFP present in the sample is bound to the wells by the immobilized antibody. The wells are washed and a primary anti-GFP detector antibody is added. After washing away unbound detector antibody, HRP-conjugated secondary detector antibody specific for the primary detector antibody is pipetted to the wells. The wells are again washed, a TMB substrate solution is added to the wells and blue colour develops in proportion to the amount of GFP bound. Finally, the concentration of GFP protein can be determined by spectrophotometrically measuring the absorbance at 600 nm. All the experiments were repeated three times in triplicate. The statistical analysis of experimental data used the Student´s t-test and the results were presented as mean ± standard deviation. Statistical significance was accepted at a level of $p < 0.05$.

2.10.3 Confocal Microscopy

Approximately 30,000 (~1mL) of N2a, HeLa and Fibroblast cells were seeded in 24-well plates previously covered with round coverslips for 24 h at 37 ºC to ensure the adhesion of the cells. After the incubation period, fresh medium was added and the cells were transfected with 500 µL of a medium-nanoparticle solution for 48 h. From here on all the steps were performed in the absence of light.

When the transfection was completed, the staining protocol began, washing the cells between each step with PBS. To stain the mitochondria, 200 µL of 200 nM MitoTracker Orange CMTMROS was added and the cells incubated for 30 min at 37 ºC. Mitotracker can only mark live-cell mitochondria, hence its addition before the fixative step.

The cells were then fixated with 4% Paraformaldehyde (PFA) for 15 min. From there on, between each step, cells were washed with PBS-T (PBS with 0.1% Tween 20). The cells were then permeabilized with PBS with 1% Triton X-100 for 10 min. To remove the auto-fluorescence of the cells, an incubation of 5min with freshly prepared PBS-NH_4Cl 50 mM was performed.

To complete the staining protocol, 200 µL of Hoescht 33342 1 µM was added to the cells and incubated for 10 min.

The lamina were mounted by placing the cell-covered lamella face-down over a drop of Entellan. The lamina were then visualized by confocal microscopy (ZEISS LSM 710, Oberkochen, Germany). Table 3 indicates the wavelengths of excitation and emission of the different probes.

Table 3 – Excitation and emission wavelengths of the different probes used in the confocal microscopy experiments

Probe	Excitation (nm)	Emission (nm)
Rhodamine 123	505	560
Hoescht 33342	343	483
Mitotracker Orange CMTMROS	554	576
EGFP	488	507

2.11 Statistical analysis

Statistical analysis and graphics design were performed using GraphPad Prism 6 software. The analysis was performed in the encapsulation test, MTT assay, cell-associated rhodamine fluorescence and GFP quantification.

Chapter 3

Results

1. Competent Cell Preparation

Cell competency was evaluated by counting the number of colonies in the plaque. Since the number of colonies exceeded 300, they were considered uncountable and thus the equation 1 could not be applied. The cells were considered highly competent.

2. Plasmid Amplification, Purification and Sequencing

Plasmids pCAG-GFP, pVAX1-*LacZ* and pcDNA3-myc-*FLNa* S2152A were amplified by fermentation and purified with a QIAGEN® Plasmid Purification kit. The first one was analysed with more detail since it was the basis of the vector we tried to create. For that, pCAG-GFP was analysed by electrophoresis to ensure that the pDNA was mainly present in the supercoiled isoform, since that is the requirement for gene therapy vectors. As it can be seen in figure 7, three bands can be observed. The first one is more diffuse while the last one is denser. Agarose gel electrophoresis works by separating nucleic acids based on their size and conformation, the longer the sequence is, the less it will travel through the matrix. In the case of pDNA, the separation observed is not based in size, since the number of base pairs of the different isoforms is the same, but by conformation. Supercoiled pDNA is a more compact form, allowing it to travel more easily through the pores of the matrix with more ease than the linear form. The open circular isoform is more retained in the gel, due to its more relaxed structure and larger hydrodynamic radius. Figure 7 then allows us to determine that the open circular isoform is almost non-existent, while the supercoiled form was the most common in the plasmid solutions.

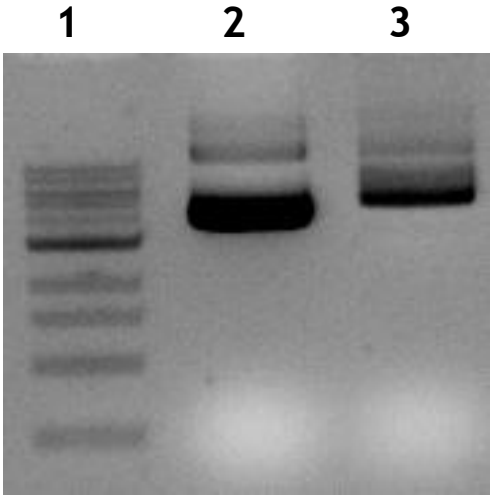

*Figure 7 - **Agarose gel electrophoresis of the purified plasmid**. Lane 1 -1 kb DNA Ladder (New England Biolab), Lane 2 - Commercial plasmid (Addgene), Lane 3 - Purified plasmid.*

Sequencing was also performed to guarantee that the plasmid obtained was pCAG-GFP. As it can be seen in figure 8, when compared the sequence provided by Addgene, plasmid 11150, to the sequence obtained for the pDNA, we observed that the amplified plasmid was indeed pCAG-GFP.

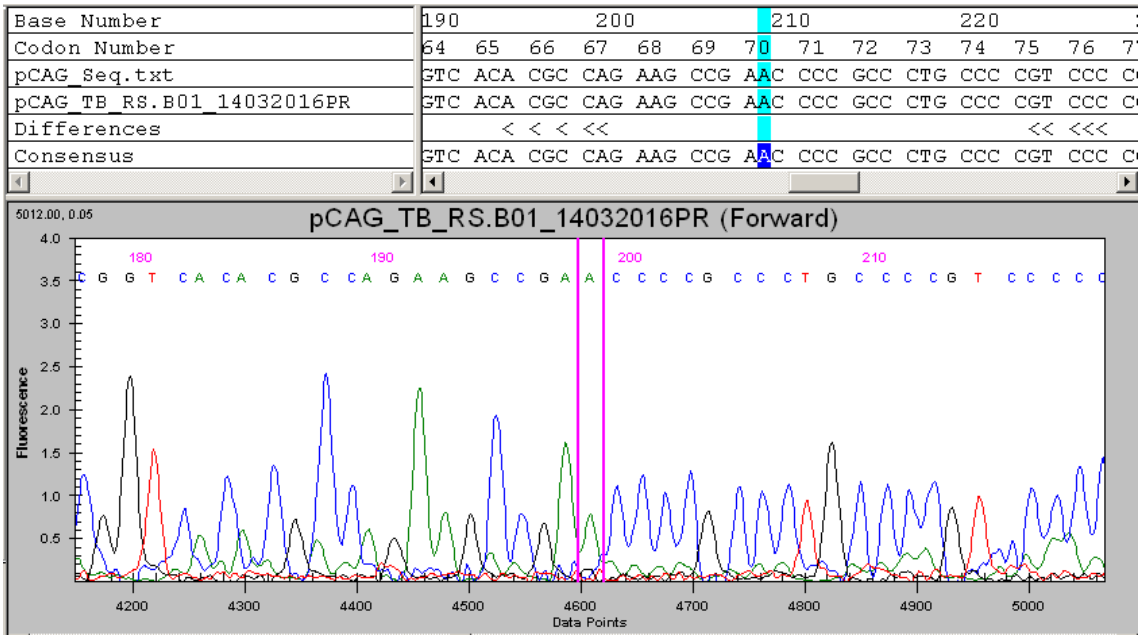

*Figure 8 - **Sequencing of the produced pCAG-GFP**. Reference sequence was obtained from Addgene plasmid 11150.*

3. ND1 amplification and *E. coli* Transformation

In our work, the focus was to isolate and amplify the mitochondrial gene ND1, a gene encoding a protein that is part of complex I of OXPHOS. For this purpose, ND1 gene was amplified from mtDNA, purified from blood samples of healthy individuals, using a PCR reaction. The PCR product was purified using GRS PCR & Gel Band Purification Kit (GRiSP, Porto, Portugal). Then, the product was analysed by agarose gel electrophoresis and sequenced, to verify its integrity, identity and purity.

Figure 9 shows the PCR products obtained. They all had the same size, slightly higher than 1 kbp, which is consistent with the ND1 gene size, approximately 1.2 kbp.

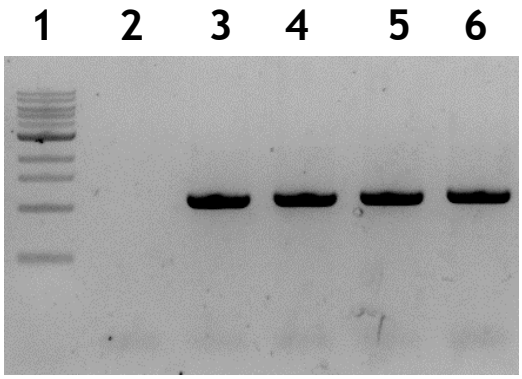

*Figure 9 - **Agarose gel electrophoresis of the amplification of ND1**. Lane 1 - 1 kb DNA Ladder, Lane 2 - Negative control, Lane 3 - Positive control (mtND1), Lane 4-6 - PCR product*

Sequencing of this product, as seen in figure 10, demonstrated that the product was indeed the ND1 gene by comparing the sequence of the mtND1 gene, obtained from GenBank, accession number NC_012920, region 3307 to 4262, to the sequence obtained from the PCR product.

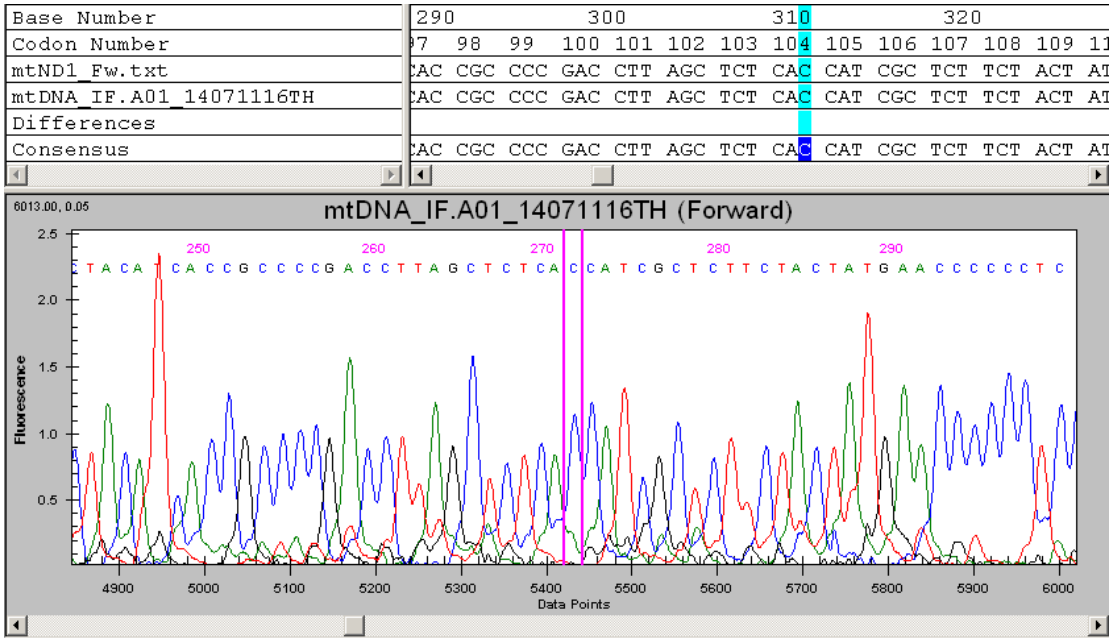

*Figure 10 - **Sequence of ND1 obtained from the PCR reaction**. The mtND1 sequence was obtained from GenBank, accession number NC_012920, region 3307 to 4262.*

E.coli JM109 were transformed with 50 ng of this new vector, pGEM®-T-mtND1, using heat shock. Several plaques were seeded, grown overnight at 37 ºC, and four were randomly chosen and one colony from each was seeded in liquid LB media to grow overnight, at 37 ºC. QIAprep Spin Miniprep Kit was used to isolate and purify the pDNA present in the cultures. The pDNA obtained was amplified by PCR and analysed by agarose gel electrophoresis.

Figure 11 shows that one culture (lane 4) had a plasmid of the same size of pGEM®-T (lane 3), while the other three cultures had a plasmid longer than the original. The difference in size is approximately 1 kb, indicating the possibility of the ND1 gene being incorporated in the pGEM®-T plasmid in cultures analysed in lanes 5, 6 and 7.

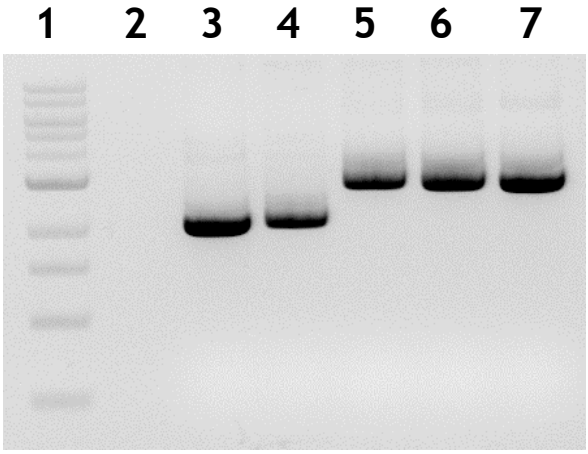

*Figure 11 - **PCR of the four cultures chosen**. Lane 1 - 1 kb DNA Ladder, Lane 2 - Negative control, Lane 3 - Positive control (pGEM®-T), Lane 4 - Culture 1, Lane 5 - Culture 2, Lane 6 - Culture 3, Lane 7 - Culture 4*

pDNA isolated from cultures 2, 3 and 4 was sequenced using primers for pGEM®-T to check the presence of the insert in the ligation product. As figure 12 shows, when comparing a theoretical sequence of the pGEM®-T-mtND1 vector, which is the plasmid sequence with the mtND1 sequence added between the T-hangs, with the sequence of the plasmid obtained from the cultures, we can observe the presence of the ND1 insert.

*Figure 12 - **Sequencing of the plasmid obtained from culture 2**. The reference sequence was adapted from the pGEM®-T sequence, by adding the sequence of mtND1 in the ligation site.*

4. Nanoparticles Production and Characterization

The nanoparticles were formed using a co-precipitation technique. The protocol was adapted from Santos and co-workers[85]. The method consisted in creating two solutions, one with $CaCl_2$, 10 µg of pDNA and rhodamine 123, solution A, and other with Na_2CO_3 and cellulose, solution B. Solution A was added dropwise to solution B to promote the formation of rhodamine pDNA based nanoparticles. Three plasmids were used, pCAG-GFP, pVAX1-*LacZ* and pcDNA3, allowing the expansion of the work previously developed. Although we were able to create a new vector, we were not able to transform *E. coli* and, therefore, not able to produce it. The work proceeded using the previously mentioned plasmids as models, and three cell lines, fibroblasts, HeLa and N2a. This gave us the opportunity to infer if different cell types reacted in a similar way to the nanoparticles and if the targeting abilities of the carriers altered in a significant way. The expression vector pCAG-GFP was also during the development of the nanoparticles, since the expressed protein GFP would allow us to follow the expression of incorporated plasmids after transfecting cells.

4.1 Morphology, size and ζ potential

Morphology of nanoparticles incorporating pCAG-GFP was evaluated using Scanning Electron Microscopy. ζ potential was determined with a Zetasizer nano ZS instrument and size was evaluated with both techniques. As it can be seen in figure 13, the nanoparticles presented a spherical shape and sizes ranging between 300 nm to 400 nm.

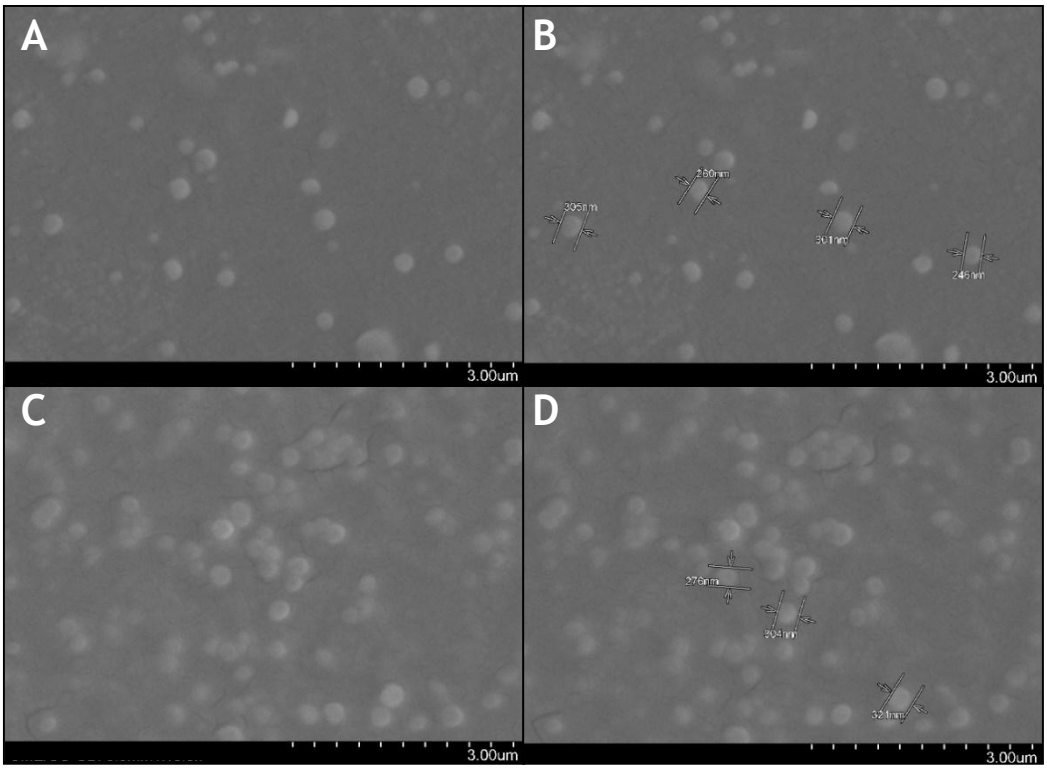

*Figure 13 - **Scanning electron micrograph of nanoparticles**. pCAG-GFP/cellulose nanoparticles (A) and size (B). pCAG-GFP/Rho/cellulose (C) and size (D).*

Negative values of ζ potential were obtained, as presented in table 4, for all plasmids and for all the pDNA/rhodamine/cellulose systems. The values obtained for the former are -40 mV for pcDNA3, -39 for pVAX1-*LacZ* and -30 mV for pCAG-GFP, and for the latter -7.6 mV for pcDNA3, -5.8 mV for pVAX1-*LacZ* and -5.3 mV for pCAG-GFP. In the absence of cellulose the values were positive, +20 mV for pcDNA3, +33 mV for pVAX1-*LacZ* and +40 mV for pCAG-GFP. Values for the ζ potential for rhodamine and cellulose are also presented. This shows that, although cellulose, and other polysaccharides, confers more stability to the nanoparticles[90], it also alters the ζ potential to a negative value, possibly reducing the nanoparticles ability to enter the cell. However, as it can be seen in topic 5, the transfection efficiency was not affected.

*Table 4 - **Average size and zeta potential of nanoparticle systems with 10 µg pDNA**. Average zeta potential values of the pDNA, free rhodamine 123 and cellulose are also presented. The values of ζ potential and size were calculated with the data obtained from three independent measurements (mean ± SD, n = 3).*

System	Particle Size (nm)	Zeta Potential (mV)
pCAG-GFP		-30 ± 0.6
pCAG-GFP/Rho/Cellulose	298 ± 9.1	-5.3 ± 0.7
pCAG-GFP/Rho	339 ± 18.2	+39.6 ±3.9
pVAX1-*LacZ*		-39 ± 0.5
pVAX1-*LacZ*/Rho/Cellulose	387.5 ± 25.5	-5.76 ± 0.3
pVAX1-*LacZ*/Rho	437 ± 28.1	+33 ± 2.4
pcDNA3		-41 ± 0.8
pcDNA3/Rho/Cellulose	386 ± 25.8	-7.65 ± 0.3
pcDNA3/Rho	441 ± 19.2	+20.4 ± 2.8
Rhodamine		+49 ± 1.3
Cellulose		-78 ± 1.8

4.2 Encapsulation Efficiency

For therapeutic purposes, the encapsulation efficiency (EE%) of the vector system must be analysed. The EE% for the nanoparticle systems under study, represented in table 5, shows that the efficiency is almost independent of pDNA size and always shows values superior to 50%. However, slightly higher encapsulation efficiency is achieved for smaller plasmids. The results indicate that the nanoparticles are capable of incorporating both pDNA and rhodamine. Figure 14 shows that rhodamine does not alter the EE% in a significant way, only decreasing it slightly. Since our objective is to target the mitochondria, the usage of rhodamine is essential, and its presence should not significantly alter the nanoparticle characteristics.

*Table 5 - **Loading efficiency of pCAG-GFP, pVAX1-LacZ and pcDNA3-based nanoparticles**. All values are represented as Mean ± SD with n = 3*

	Loading efficiency (%)
	pDNA
pCAG-GFP	66 ± 1.3
pVAX1-*LacZ*	57 ± 1.4
pcDNA3	51 ± 0.9

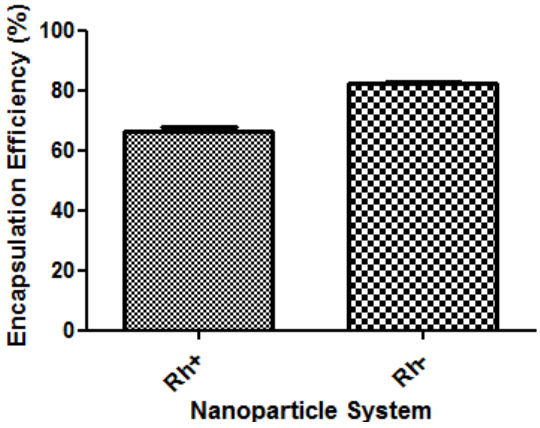

*Figure 14 - **Encapsulation Efficiency of CaCO3-pDNA-Rho123 Nanoparticles**. All values are represented as Mean ± SEM with N=9 for Rh+ and N=6 for Rh-.*

4.3 Cell Cytotoxicity

MTT is a yellow, water-soluble, tetrazolium salt. The MTT assay is a simple non-radioactive colorimetric assay to measure cell cytotoxicity or viability. Metabolically active cells are able to convert this dye into a water-insoluble dark blue formazan by reductive cleavage of the tetrazolium ring. The formed crystals can be dissolved and quantified by measuring the absorbance of the solution at 570 nm. The results, as observed in figure 15, suggest that the nanoparticles are not significantly toxic to cells, and thus, do not have significant cytotoxic effect. Both systems, with and without rhodamine, present a viability of approximately 82% and 81%, respectively, after 24 h, and 81% after 48 h.

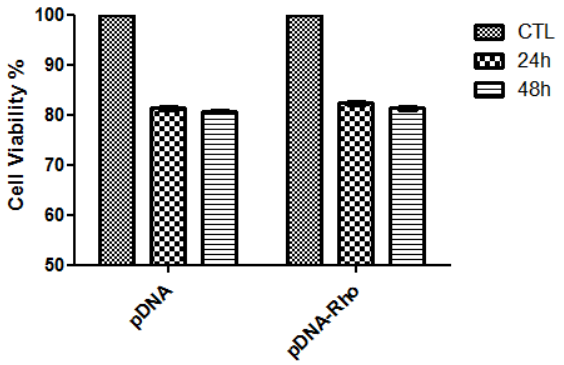

*Figure 15 - **Cell Viability after incubation for 24h and 48h of Fibroblast cells with CaCO3-pDNA and CaCO3-pDNA-Rho123 nanoparticles for pCAG-GFP**. All values are represented as Mean ± SEM with N=3 followed by a Two-way Anova treatment, * p<0.05 when compared to control. Control was defined as 100% Cell Viability*

5. Transfection studies

5.1 Cell-associated rhodamine fluorescence

To demonstrate pDNA rhodamine based nanoparticles cell uptake, the fluorescence intensity of rhodamine 123 in fibroblast and tumoral cells has been quantified after cell transfection with pcDNA3-based nanoparticles at different time periods. From the presented data, it is possible to confirm the uptake of nanoparticles in all cell lines and verify that the cell-associated fluorescence is time dependent. The internalization of nanoparticles is denoted by a gradual increase in rhodamine fluorescence until 24 hours of transfection; at this time, a plateau is attained. Although the observed pattern is quite similar for the different cell lines under study, we found a larger cell fluorescence intensity in neuroblastoma cells for all times of transfection. As can be seen in figure 16, the rhodamine cell-associated fluorescence confirms the nanoparticles uptake and internalization.

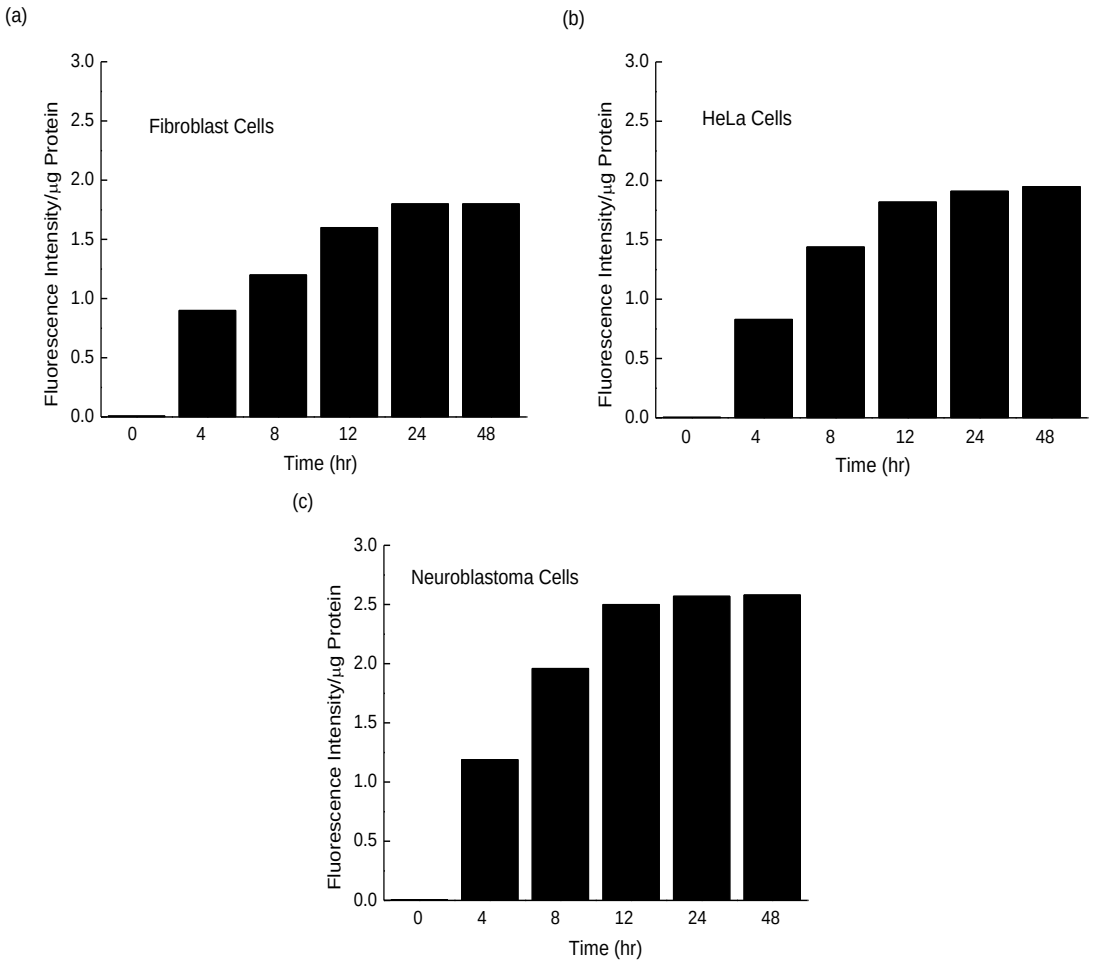

*Figure 16 - **Cell-associated rhodamine fluorescence**. Rhodamine fluorescence intensity in (a) fibroblast, (b) HeLa cancer and (c) neuroblastoma cells after 4, 8, 12, 24 and 48 hours of transfection with rhodamine pcDNA3 based nanoparticles. The data were obtained by calculating the average of 3 experiments. The respective errors were determined and were below 0.05%.*

5.2 GFP Quantification

Internalization of the pCAG-GFP based nanoparticles was also evaluated by quantifying the expression of GFP protein. As it can be seen in figure 17, the transfection mediated by pCAG-GFP nanoparticles, in the absence of rhodamine, results in the expression of GFP. A fluorescence confocal microscopy analysis confirms the GFP protein expression in fibroblast cells when transfection is mediated by the same nanoparticles, as presented in figure 18. When rhodamine is incorporated into nanoparticles, they are targeted to mitochondria where GFP cannot be expressed. This is due to the different genetic code and, therefore, demonstrates the mitochondrial targeting ability of rhodamine pDNA nanoparticles.

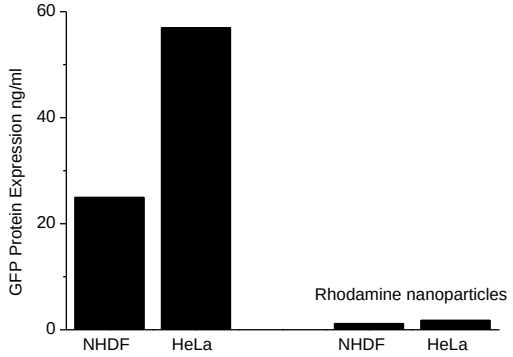

*Figure 17 - **Quantification of GFP**. Quantification of GFP protein expression in NHDF and HeLa cells using a GFP ELISA kit, after 48 hours of transfection with pCAG-GFP/cellulose nanoparticles (left side) and pCAG-GFP/Rho/cellulose nanoparticles (right side).*

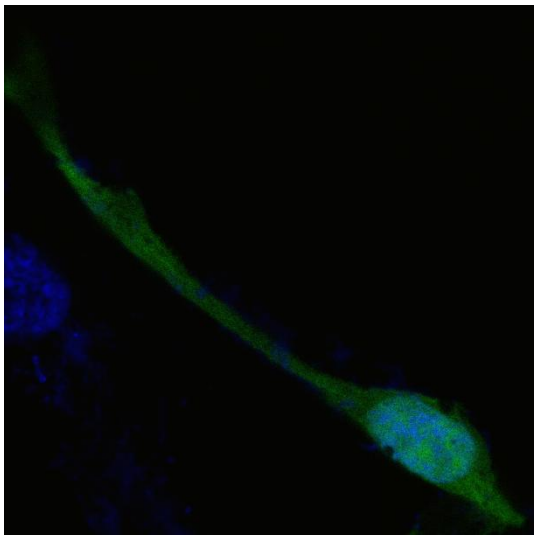

Figure 18 - Fluorescence confocal microscopy analysis of GFP expression after fibroblast cells transfection mediated by pCAG-GFP/cellulose nanoparticles; nucleus has been stained blue by Hoescht 33342.

5.3 Confocal Microscopy

Confocal microscopy was used to evaluate the internalization of pcDNA3, pVAX1-*LacZ* and pCAG-GFP based nanoparticles. The first two were not studied with fibroblasts since they were already tested in these cells[85]. pCAG-GFP nanoparticles were only evaluated in fibroblast in the absence of rhodamine. Due to the low transfection efficiency/low expression of GFP further studies were not possible.

Nanocarrier mediated delivery has been investigated by fluorescence confocal microscopy in a study where nucleus and mitochondrion have been stained with adequate fluorescent dyes. Figures 19 and 20 show that there is co-localization of nanoparticles, stained in green, and mitochondria, stained in orange, as verified by the yellow colour present in the merged image. The results support the idea that the nanoparticles have no significant difference in transfection efficiency when using different plasmids or cell types.

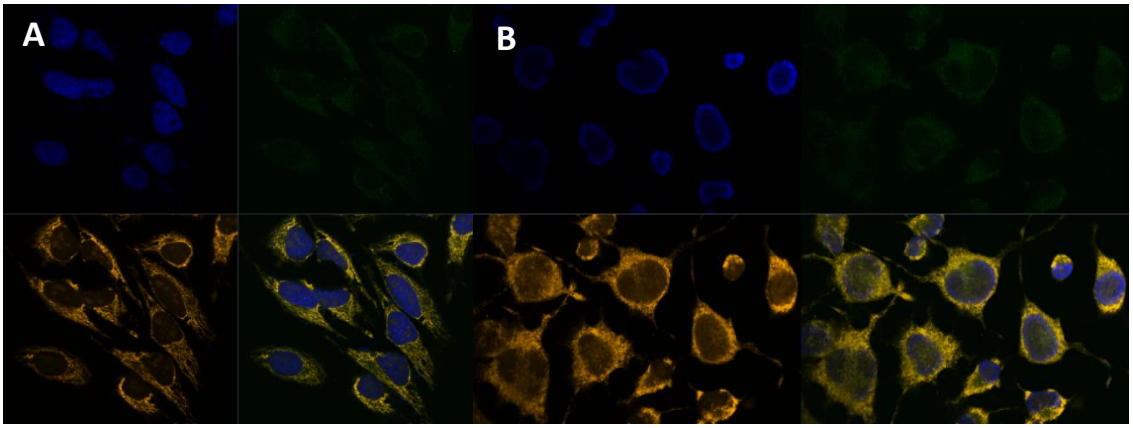

*Figure 19 - **Confocal images of transfection studies with pcDNA3-Rhodamine nanoparticles**. A - HeLa cells, B - N2a cells. Nuclei were stained with Hoescht 33342 (blue), mitochondria with Mitotracker Orange(orange), rhodamine was incorporated in the nanoparticles (green).*

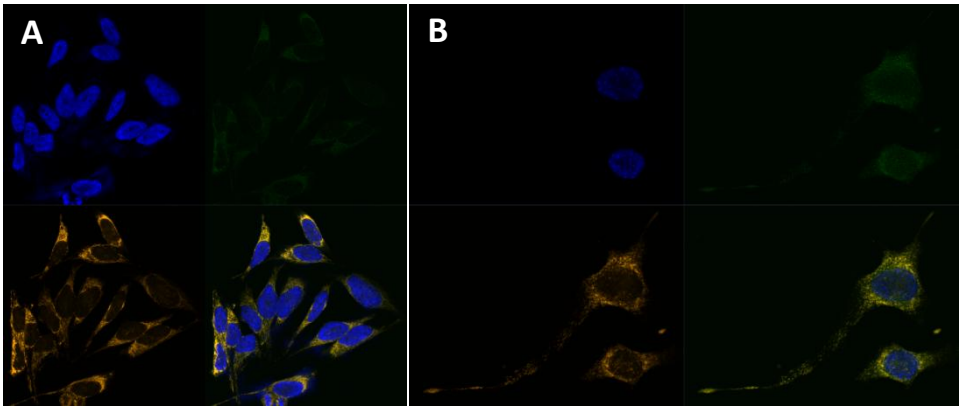

*Figure 20 - **Confocal images of transfection studies with pVAX1-**LacZ**-Rhodamine nanoparticles**. A - HeLa cells, B - N2a cells. Nuclei were stained with Hoescht 33342 (blue), mitochondria with Mitotracker Orange(orange), rhodamine was incorporated in the nanoparticles (green).*

Figure 21, showing a Z-plane analysis, further confirms the mitochondrial targeting ability of rhodamine pDNA based nanoparticles.

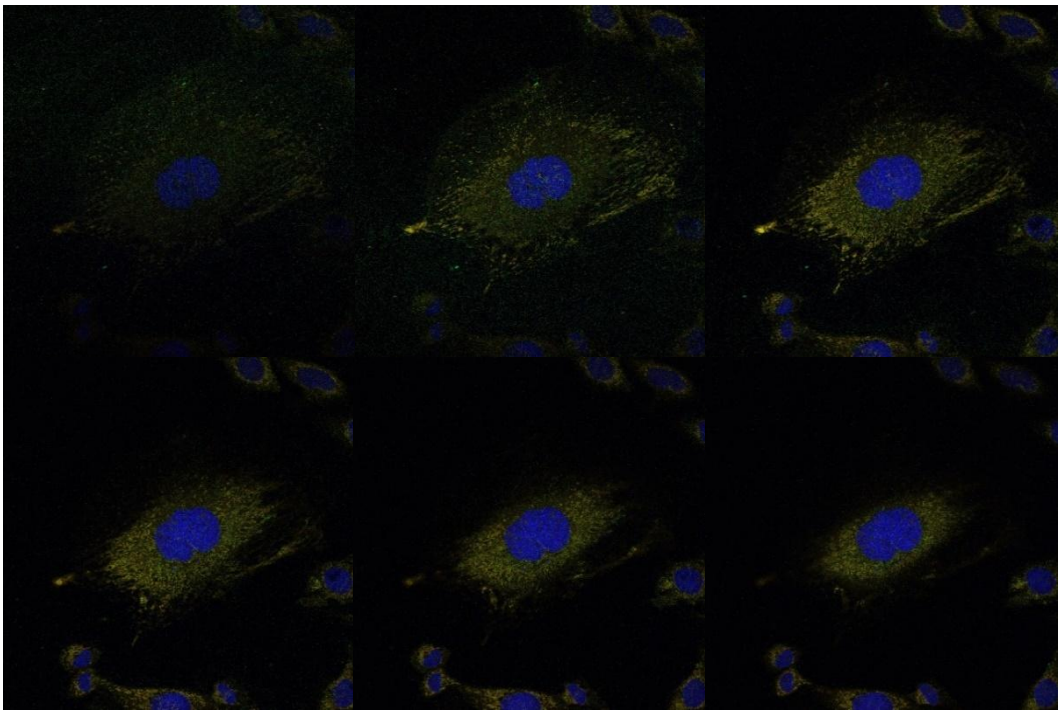

*Figure 21 - **Three-dimensional Z-plane analysis of the co-localization of mitochondria and pVAX1-LacZ/ Rho/cellulose nanoparticles in fibroblast cells**. Nucleus stained blue by Hoescht 33342 and mitochondria stained orange by Mitotracker Orange. pVAX1-*LacZ*/ Rho/cellulose nanoparticles stained green. Merged image presentation.*

Chapter 4

Discussion

Gene therapy has been extensively studied in the last years due to the possibilities that it offers in the treatment of genetic diseases. Mitochondrial cytopathies, however, do not have yet an efficient treatment, and gene therapy appears as a promising approach for such mitochondrial DNA disorders. There is lack of a vector containing mitochondrial genes that can be used in these treatments, and the recent studies have been mainly focusing in the amplification of the entire mtDNA[86, 88] or in the use of viral vectors[78]. In this dissertation, we demonstrate the development of a new vector containing the ND1 gene, a gene that encodes one of the proteins of the complex I of the OXPHOS, and a suitable non-viral nanocarrier capable of cell uptake, internalization and mitochondria targeting.

In order to amplify the plasmids used, competent cells were prepared. These cells have the ability to take in foreign DNA, and the cells we selected, *E. coli* JM109, have certain characteristics removed, like endonucleases that degrade DNA.

We used a protocol, inspired by Inoue's et al. protocol, which allowed us to prepare highly competent cells, as demonstrated by the high number of colonies that grew after transformation.

These cells were then transformed using pCAG-GFP, an expression plasmid selected for this study, lysed and the pDNA purified. High yields were obtained, and the plasmid obtained was mostly in supercoiled isoform. Sequencing of the pDNA obtained allowed us to confirm that it was indeed pCAG-GFP that we amplified.

Amplification of our gene of interest was carried using PCR, and the PCR product purified. Ligation of the gene was made in pGEM®-T, as confirmed by colony-PCR and sequencing. This shows that it is indeed possible to clone isolated mitochondrial genes, opening the way for further studies on human mitochondrial genome cloning.

Due to our interest to create a vector containing both a mitochondrial gene and a reporter gene, we tried to ligate the mtND1 to pGAC-GFP. However, despite our best efforts, we were not able to create a vector using this plasmid.

Rhodamine plasmid DNA based nanoparticles were prepared by a co-precipitation method. Three different nanoparticle systems were produced by using three plasmids, pCAG-GFP, pcDNA3 and pVAX1-*LacZ*, and by incorporating rhodamine 123, a fluorescent dye with affinity

to the mitochondria, in order to allow the carriers to target this organelle. To reduce the size, improve the stability and augment the transfection efficiency of the nanoparticles, cellulose was added.

Scanning electron microscopy allowed us to verify that the nanoparticles, independently of the pDNA used, have a spherical form and a small size, 300 nm for the pCAG-GFP system and approximately 390 nm for the pVAX1-*LacZ* and pcDNA3 systems, as confirmed by the use of a Zetasizer. The studies also show that the use of cellulose reduces the average size of the carriers. This demonstrates that the carriers are appropriate for transfection studies due their small size. Zeta potential was negative in all the systems, with values ranging the -5 mV for the pCAG-GFP and the pVAX1-*LacZ* systems, and -7.6 mV for the pcDNA3 system. These negative values are caused by the use of cellulose, since in the absence of the polysaccharide the values are positive, ranging from +40 mV for the pCAG-GFP system and +20 mV for the pcDNA3 system. Although it reduces the size of the nanoparticles, the low ζ potential of the compound also reduces the ζ potential of the carriers. This can influence the transfection efficiency, by making the interaction with the cellular membrane harder. However, from the *in vitro* studies, transfection efficiency was confirmed to be unaltered.

Besides size and morphology, loading capacity and cytotoxicity must also be evaluated in order to design a suitable gene delivery system. Encapsulation efficiency of pDNA in all the systems, in the presence of rhodamine 123, was above 50%, the highest being in the pCAG-GFP system. The influence of the incorporation of rhodamine in the encapsulation was also evaluated, and we verified that in the absence of the dye, the efficiency is approximately 80%. Nonetheless, the efficiency is high enough for the nanoparticles to be considered appropriate for gene therapy.

MTT assay was performed to analyse the cytotoxicity of the nanoparticles in fibroblast cells after 24 h and 48 h of transfection. The results show that the pCAG-GFP system is not significantly toxic to the cells, suggesting that no immune response should be triggered when using these nanoparticles.

Rhodamine fluorescence was quantified in the transfected cells at different times in different cell lines using the pCAG-GFP/Rho/Cellulose system. The fluorescence increased until 24 h after transfection in all cell lines, but the intensity was higher in neuroblastoma cells. This allows us to conclude that the nanoparticles are being internalised by the cells.

Knowing this, the next step was to test the targeting ability of the nanocarriers for the mitochondria. The results show that GFP is only expressed when using the nanoparticles developed in the absence of rhodamine; confocal microscopy studies also show the expression of GFP is achieved when using the rhodamine-free system.

No expression of GFP protein has been observed when cell transfection is mediated by rhodamine pDNA nanoparticles. This system targets mitochondria and the lack of GFP expression is due to the differences of the genetic code of this organelle.

Confocal microscopy studies using different cell lines, such as, fibroblasts and tumoral cells also indicate the targeting ability displayed by rhodamine pDNA nanoparticles. The merged images show that the nanoparticles are present in the mitochondria due to the yellow colour, a mixture of the green from the rhodamine and the orange from the MitoTracker Orange, which appears inside the cells. Moreover, two and three dimensional fluorescence confocal microscopy studies confirm mitochondrial localization of pDNA based systems.

When comparing the different plasmids used, we can verify that the characteristics, transfection efficiency and mitochondrial targeting ability of the nanoparticles is independent of the type and size of the genetic vector. This reflects the adequacy of the pDNA developed nanoparticle systems for gene therapy. Although plasmid DNA delivery to the mitochondrial matrix is not yet strongly demonstrated, our results truly show the mitochondrial targeting ability of pDNA/rhodamine vectors.

Conclusions and Future Perspectives

Mitochondrial gene therapy is still a recent field of study, but the applications in the treatment of many diseases increases every day. However, the development of a safe and effective method of delivering a gene to the mitochondria is still in the early stages.

We were able to clone a single gene from mtDNA in pGEM®-T, opening the way to the development of new vectors that incorporate mitochondrial genes. However, we were not successful in creating an mtDNA vector with a reporter gene, although preliminary studies are promising.

We were also able to develop nanoparticles capable of targeting the mitochondria using a fluorescent dye, rhodamine 123, with affinity for that organelle. The plasmids (pCAG-GFP, pcDNA3 and pVAX1-*LacZ*) used to create the nanoparticles do not seem to affect the characteristics of the carriers. All the systems presented a small size, high encapsulation of pDNA and low cytotoxicity, making them appropriate for gene therapy.

The different carriers can also be internalized by diverse cell lines, fibroblasts, HeLa and N2a, and are able to target the mitochondria when the nanoparticles incorporate rhodamine. Inexpression of GFP in cells transfected with the pCAG-GFP nanoparticle system suggests that the carriers are able to deliver pDNA to the mitochondria.

Although gene expression into mitochondria was not demonstrated in this work, the developed pDNA systems represent a valuable tool to be used in mitochondrial gene therapy

purposes. Supported mainly by the in vitro studies, the findings described in this thesis are a great hallmark in this poorly studied area.

Mitochondrial DNA disorders demand a continuous search of a suitable mitochondrial targeted vector. In line with this, future work should put a lot of emphasis in the development of a mitochondrial gene delivery system for human mitochondrial gene therapy implementation contributing for new therapies centred in mitochondria. Further studies should focus on the construction of an expression plasmid containing a mitochondrial gene and the expression of the delivered genes should be evaluated *in vitro*. If the nanoparticles are shown to be an efficient mitochondrial gene delivery system, *in vivo* studies could be initiated.

Bibliography

1. Penta J. S., Johnson F. M., Wachsman J. T., Copeland W. C. Mitochondrial DNA in human malignancy. *Mutation research*. 2001; 488(2):119-33.

2. Lander E. S. Initial impact of the sequencing of the human genome. *Nature*. 2011; 470(7333):187-97.

3. Venter J. C., Adams M. D., Myers E. W., Li P. W., Mural R. J., Sutton G. G., et al. The sequence of the human genome. *Science*. 2001; 291(5507):1304-51.

4. Clark J., Dai Y., Simon D. K. Do somatic mitochondrial DNA mutations contribute to Parkinson's disease? *Parkinsons Dis*. 2011; 2011:659694.

5. Byrne E. M., McRae A. F., Duffy D. L., Zhao Z. Z., Martin N. G., Whitfield J. B., et al. Family-based mitochondrial association study of traits related to type 2 diabetes and the metabolic syndrome in adolescents. *Diabetologia*. 2009; 52(11):2359-68.

6. Sharma H., Singh A., Sharma C., Jain S. K., Singh N. Mutations in the mitochondrial DNA D-loop region are frequent in cervical cancer. *Cancer Cell Int*. 2005; 5:34.

7. Simon D. K., Johns D. R. Mitochondrial disorders: clinical and genetic features. *Annu Rev Med*. 1999; 50:111-27.

8. Wallace D. C. Diseases of the mitochondrial DNA. *Annu Rev Biochem*. 1992; 61:1175-212.

9. Elliott H. R., Samuels D. C., Eden J. A., Relton C. L., Chinnery P. F. Pathogenic mitochondrial DNA mutations are common in the general population. *Am J Hum Genet*. 2008; 83(2):254-60.

10. Greaves L. C., Reeve A. K., Taylor R. W., Turnbull D. M. Mitochondrial DNA and disease. *The Journal of pathology*. 2012; 226(2):274-86.

11. Wirth T., Parker N., Yla-Herttuala S. History of gene therapy. *Gene*. 2013; 525(2):162-9.

12. Limberis M. P. Phoenix rising: gene therapy makes a comeback. *Acta biochimica et biophysica Sinica*. 2012; 44(8):632-40.

13. Gray M. W., Burger G., Lang B. F. Mitochondrial evolution. *Science*. 1999; 283(5407):1476-81.

14. Scheffler I. E. Mitochondria make a come back. *Adv Drug Deliver Rev*. 2001; 49(1-2):3-26.

15. Rich P. R., Marechal A. The mitochondrial respiratory chain. *Essays in biochemistry*. 2010; 47:1-23.

16. Flindt R. Amazing Numbers in Biology. Berlin, Heidelberg: Springer Berlin Heidelberg; 2006.

17. Krauss S. Mitochondria: Structure and Role in Respiration. eLS: John Wiley & Sons, Ltd; 2001.

18. Zick M., Rabl R., Reichert A. S. Cristae formation-linking ultrastructure and function of mitochondria. *Biochim Biophys Acta*. 2009; 1793(1):5-19.

19. Nunnari J., Suomalainen A. Mitochondria: in sickness and in health. *Cell*. 2012; 148(6):1145-59.

20. Piomboni P., Focarelli R., Stendardi A., Ferramosca A., Zara V. The role of mitochondria in energy production for human sperm motility. *International journal of andrology*. 2012; 35(2):109-24.

21. Hoefs S. J., Rodenburg R. J., Smeitink J. A., van den Heuvel L. P. Molecular base of biochemical complex I deficiency. *Mitochondrion*. 2012; 12(5):520-32.

22. Lehninger A. L., Nelson D. L., Cox M. M. Lehninger principles of biochemistry. 5th ed. New York: W.H. Freeman; 2008.

23. Chaban Y., Boekema E. J., Dudkina N. V. Structures of mitochondrial oxidative phosphorylation supercomplexes and mechanisms for their stabilisation. *Biochim Biophys Acta*. 2014; 1837(4):418-26.

24. Quinlan C. L., Orr A. L., Perevoshchikova I. V., Treberg J. R., Ackrell B. A., Brand M. D. Mitochondrial complex II can generate reactive oxygen species at high rates in both the forward and reverse reactions. *J Biol Chem*. 2012; 287(32):27255-64.

25. Yu E. P., Bennett M. R. Mitochondrial DNA damage and atherosclerosis. *Trends in endocrinology and metabolism: TEM*. 2014; 25(9):481-7.

26. Sena L. A., Chandel N. S. Physiological roles of mitochondrial reactive oxygen species. *Molecular cell*. 2012; 48(2):158-67.

27. Venditti P., Di Stefano L., Di Meo S. Mitochondrial metabolism of reactive oxygen species. *Mitochondrion*. 2013; 13(2):71-82.

28. Kowaltowski A. J., de Souza-Pinto N. C., Castilho R. F., Vercesi A. E. Mitochondria and reactive oxygen species. *Free radical biology & medicine*. 2009; 47(4):333-43.

29. Pung Y. F., Sam W. J., Hardwick J. P., Yin L., Ohanyan V., Logan S., et al. The role of mitochondrial bioenergetics and reactive oxygen species in coronary collateral growth. *American journal of physiology Heart and circulatory physiology*. 2013; 305(9):H1275-80.

30. Clapham D. E. Calcium signaling. *Cell*. 2007; 131(6):1047-58.

31. Rizzuto R., De Stefani D., Raffaello A., Mammucari C. Mitochondria as sensors and regulators of calcium signalling. *Nature reviews Molecular cell biology*. 2012; 13(9):566-78.

32. Szabadkai G., Duchen M. R. Mitochondria: the hub of cellular Ca2+ signaling. *Physiology*. 2008; 23:84-94.

33. Mattson M. P., Chan S. L. Calcium orchestrates apoptosis. *Nature cell biology*. 2003; 5(12):1041-3.

34. Green D. R., Reed J. C. Mitochondria and apoptosis. *Science*. 1998; 281(5381):1309-12.

35. West A. P., Shadel G. S., Ghosh S. Mitochondria in innate immune responses. *Nature reviews Immunology*. 2011; 11(6):389-402.

36. Cloonan S. M., Choi A. M. Mitochondria: commanders of innate immunity and disease? *Current opinion in immunology*. 2012; 24(1):32-40.

37. Arnoult D., Soares F., Tattoli I., Girardin S. E. Mitochondria in innate immunity. *EMBO reports*. 2011; 12(9):901-10.

38. Collombet J. M., Coutelle C. Towards gene therapy of mitochondrial disorders. *Mol Med Today*. 1998; 4(1):31-8.

39. D'Souza G. G., Boddapati S. V., Weissig V. Gene therapy of the other genome: the challenges of treating mitochondrial DNA defects. *Pharmaceutical research*. 2007; 24(2):228-38.

40. Kagawa Y., Inoki Y., Endo H. Gene therapy by mitochondrial transfer. *Adv Drug Deliv Rev*. 2001; 49(1-2):107-19.

41. Tao M., You C. P., Zhao R. R., Liu S. J., Zhang Z. H., Zhang C., et al. Animal mitochondria: evolution, function, and disease. *Current molecular medicine*. 2014; 14(1):115-24.

42. St John J. The control of mtDNA replication during differentiation and development. *Biochim Biophys Acta*. 2014; 1840(4):1345-54.

43. Schon E. A., DiMauro S., Hirano M. Human mitochondrial DNA: roles of inherited and somatic mutations. *Nature reviews Genetics*. 2012; 13(12):878-90.

44. Schwartz M., Vissing J. Paternal inheritance of mitochondrial DNA. *The New England journal of medicine*. 2002; 347(8):576-80.

45. Chinnery P. F., Hudson G. Mitochondrial genetics. *British medical bulletin*. 2013; 106:135-59.

46. Sutovsky P. Ubiquitin-dependent proteolysis in mammalian spermatogenesis, fertilization, and sperm quality control: killing three birds with one stone. *Microscopy research and technique*. 2003; 61(1):88-102.

47. Muftuoglu M., Mori M. P., de Souza-Pinto N. C. Formation and repair of oxidative damage in the mitochondrial DNA. *Mitochondrion*. 2014; 17:164-81.

48. Cline S. D. Mitochondrial DNA damage and its consequences for mitochondrial gene expression. *Biochim Biophys Acta*. 2012; 1819(9-10):979-91.

49. Bratic A., Larsson N. G. The role of mitochondria in aging. *The Journal of clinical investigation*. 2013; 123(3):951-7.

50. Lee H. C., Wei Y. H. Mitochondria and aging. *Advances in experimental medicine and biology*. 2012; 942:311-27.

51. Mazunin I. O., Volodko N. V., Starikovskaya E. B., Sukernik R. I. Mitochondrial genome and human mitochondrial diseases. *Mol Biol*. 2010; 44(5):665-81.

52. Pearce S., Nezich C. L., Spinazzola A. Mitochondrial diseases: translation matters. *Molecular and cellular neurosciences*. 2013; 55:1-12.

53. Thambisetty M., Newman N. J. Diagnosis and management of MELAS. *Expert review of molecular diagnostics*. 2004; 4(5):631-44.

54. Cohen B. H. Neuromuscular and systemic presentations in adults: diagnoses beyond MERRF and MELAS. *Neurotherapeutics : the journal of the American Society for Experimental NeuroTherapeutics*. 2013; 10(2):227-42.

55. Pavlakis S. G., Phillips P. C., DiMauro S., De Vivo D. C., Rowland L. P. Mitochondrial myopathy, encephalopathy, lactic acidosis, and strokelike episodes: a distinctive clinical syndrome. *Ann Neurol*. 1984; 16(4):481-8.

56. Goto Y., Nonaka I., Horai S. A mutation in the tRNA(Leu)(UUR) gene associated with the MELAS subgroup of mitochondrial encephalomyopathies. *Nature*. 1990; 348(6302):651-3.

57. Finsterer J. Inherited mitochondrial neuropathies. *Journal of the neurological sciences*. 2011; 304(1-2):9-16.

58. Fukuhara N., Tokiguchi S., Shirakawa K., Tsubaki T. Myoclonus epilepsy associated with ragged-red fibres (mitochondrial abnormalities): disease entity or a syndrome? Light-and electron-microscopic studies of two cases and review of literature. *Journal of the neurological sciences*. 1980; 47(1):117-33.

59. Shoffner J. M., Lott M. T., Lezza A. M., Seibel P., Ballinger S. W., Wallace D. C. Myoclonic epilepsy and ragged-red fiber disease (MERRF) is associated with a mitochondrial DNA tRNA(Lys) mutation. *Cell*. 1990; 61(6):931-7.

60. Leber T. Ueber hereditäre und congenital-angelegte Sehnervenleiden. *Graefe's Arhiv für Ophthalmologie*. 1871; 17(2):249-91.

61. Finsterer J. Parkinson's syndrome and Parkinson's disease in mitochondrial disorders. *Movement disorders : official journal of the Movement Disorder Society*. 2011; 26(5):784-91.

62. Kosel S., Grasbon-Frodl E. M., Mautsch U., Egensperger R., von Eitzen U., Frishman D., et al. Novel mutations of mitochondrial complex I in pathologically proven Parkinson disease. *Neurogenetics*. 1998; 1(3):197-204.

63. Ibraheem D., Elaissari A., Fessi H. Gene therapy and DNA delivery systems. *International journal of pharmaceutics*. 2014; 459(1-2):70-83.

64. Blaese R. M., Culver K. W., Chang L., Anderson W. F., Mullen C., Nienhuis A., et al. Treatment of severe combined immunodeficiency disease (SCID) due to adenosine deaminase deficiency with CD34+ selected autologous peripheral blood cells transduced with a human ADA gene. Amendment to clinical research project, Project 90-C-195, January 10, 1992. *Human gene therapy*. 1993; 4(4):521-7.

65. High K. A., Aubourg P. rAAV human trial experience. *Methods in molecular biology*. 2011; 807:429-57.

66. Vannucci L., Lai M., Chiuppesi F., Ceccherini-Nelli L., Pistello M. Viral vectors: a look back and ahead on gene transfer technology. *The new microbiologica*. 2013; 36(1):1-22.

67. Pezzoli D., Chiesa R., De Nardo L., Candiani G. We still have a long way to go to effectively deliver genes! *Journal of applied biomaterials & functional materials*. 2012; 10(2):82-91.

68. Wang W., Li W., Ma N., Steinhoff G. Non-viral gene delivery methods. *Curr Pharm Biotechnol*. 2013; 14(1):46-60.

69. Olton D., Li J., Wilson M. E., Rogers T., Close J., Huang L., et al. Nanostructured calcium phosphates (NanoCaPs) for non-viral gene delivery: influence of the synthesis parameters on transfection efficiency. *Biomaterials*. 2007; 28(6):1267-79.

70. Cheang T. Y., Wang S. M., Hu Z. J., Xing Z. H., Chang G. Q., Yao C., et al. Calcium carbonate/CaIP6 nanocomposite particles as gene delivery vehicles for human vascular smooth muscle cells. *Journal of Materials Chemistry*. 2010; 20(37):8050-5.

71. Chen S., Li F., Zhuo R. X., Cheng S. X. Efficient non-viral gene delivery mediated by nanostructured calcium carbonate in solution-based transfection and solid-phase transfection. *Mol Biosyst*. 2011; 7(10):2841-7.

72. Weiss M. J., Wong J. R., Ha C. S., Bleday R., Salem R. R., Steele G. D., Jr., et al. Dequalinium, a topical antimicrobial agent, displays anticarcinoma activity based on selective mitochondrial accumulation. *Proc Natl Acad Sci U S A*. 1987; 84(15):5444-8.

73. D'Souza G. G., Rammohan R., Cheng S. M., Torchilin V. P., Weissig V. DQAsome-mediated delivery of plasmid DNA toward mitochondria in living cells. *Journal of controlled release : official journal of the Controlled Release Society*. 2003; 92(1-2):189-97.

74. Weissig V., D'Souza G. G., Torchilin V. P. DQAsome/DNA complexes release DNA upon contact with isolated mouse liver mitochondria. *Journal of controlled release : official journal of the Controlled Release Society*. 2001; 75(3):401-8.

75. Weissig V., Lizano C., Torchilin V. P. Selective DNA release from DQAsome/DNA complexes at mitochondria-like membranes. *Drug delivery*. 2000; 7(1):1-5.

76. Lyrawati D., Trounson A., Cram D. Expression of GFP in the mitochondrial compartment using DQAsome-mediated delivery of an artificial mini-mitochondrial genome. *Pharmaceutical research*. 2011; 28(11):2848-62.

77. Weissig V., Boddapati S. V., Cheng S. M., D'Souza G. G. Liposomes and liposome-like vesicles for drug and DNA delivery to mitochondria. *Journal of liposome research*. 2006; 16(3):249-64.

78. Yu H., Koilkonda R. D., Chou T. H., Porciatti V., Ozdemir S. S., Chiodo V., et al. Gene delivery to mitochondria by targeting modified adenoassociated virus suppresses Leber's hereditary optic neuropathy in a mouse model. *Proc Natl Acad Sci U S A*. 2012; 109(20):E1238-47.

79. Flemming A. Gene therapy: Crossing mitochondrial barriers. *Nature reviews Drug discovery*. 2012; 11(6):439.

80. Yamada Y., Akita H., Kamiya H., Kogure K., Yamamoto T., Shinohara Y., et al. MITO-Porter: A liposome-based carrier system for delivery of macromolecules into mitochondria via membrane fusion. *Biochim Biophys Acta*. 2008; 1778(2):423-32.

81. Yamada Y., Furukawa R., Yasuzaki Y., Harashima H. Dual function MITO-Porter, a nano carrier integrating both efficient cytoplasmic delivery and mitochondrial macromolecule delivery. *Mol Ther*. 2011; 19(8):1449-56.

82. Yamada Y., Harashima H. Delivery of bioactive molecules to the mitochondrial genome using a membrane-fusing, liposome-based carrier, DF-MITO-Porter. *Biomaterials*. 2012; 33(5):1589-95.

83. Yamada Y., Nakamura K., Furukawa R., Kawamura E., Moriwaki T., Matsumoto K., et al. Mitochondrial delivery of bongkrekic acid using a MITO-Porter prevents the induction of apoptosis in human HeLa cells. *Journal of pharmaceutical sciences*. 2013; 102(3):1008-15.

84. Yasuzaki Y., Yamada Y., Harashima H. Mitochondrial matrix delivery using MITO-Porter, a liposome-based carrier that specifies fusion with mitochondrial membranes. *Biochem Biophys Res Commun*. 2010; 397(2):181-6.

85. Santos J., Sousa F., Queiroz J., Costa D. Rhodamine based plasmid DNA nanoparticles for mitochondrial gene therapy. *Colloids and surfaces B, Biointerfaces*. 2014; 121:129-40.

86. Tapper D. P., Van Etten R. A., Clayton D. A. Isolation of mammalian mitochondrial DNA and RNA and cloning of the mitochondrial genome. *Methods in enzymology*. 1983; 97:426-34.

87. Yoon Y. G., Koob M. D. Efficient cloning and engineering of entire mitochondrial genomes in Escherichia coli and transfer into transcriptionally active mitochondria. *Nucleic Acids Research*. 2003; 31(5):1407-15.

88. Bigger B. W., Liao A. Y., Sergijenko A., Coutelle C. Trial and error: how the unclonable human mitochondrial genome was cloned in yeast. *Pharmaceutical research*. 2011; 28(11):2863-70.

89. Inoue H., Nojima H., Okayama H. High efficiency transformation of Escherichia coli with plasmids. *Gene*. 1990; 96(1):23-8.

90. Zhao D., Zhuo R. X., Cheng S. X. Alginate modified nanostructured calcium carbonate with enhanced delivery efficiency for gene and drug delivery. *Mol Biosyst*. 2012; 8(3):753-9.